Earth-Science Reviews 180 (2018) 37–59

Contents lists available at ScienceDirect

Earth-Science Reviews

journal homepage: www.elsevier.com/locate/earscirev

# Palaeogeographic evolution of the late Miocene Rifian Corridor (Morocco): Reconstructions from surface and subsurface data

W. Capella[a,*], N. Barhoun[b], R. Flecker[c], F.J. Hilgen[a], T. Kouwenhoven[a], L.C. Matenco[a], F.J. Sierro[d], M.A. Tulbure[a], M.Z. Yousfi[e], W. Krijgsman[a]

[a] Department of Earth Sciences, Utrecht University, 3584CD, Utrecht, The Netherlands
[b] Université Hassan II Mohammedia, Fac. Sci. Ben M'Sik, BP7955 Casablanca, Morocco
[c] BRIDGE, School of Geographical Sciences and Cabot Institute, University of Bristol, Bristol BS8 1SS, UK
[d] Department of Geology, University of Salamanca, 37008 Salamanca, Spain
[e] ONHYM, 10050 Rabat, Morocco

ARTICLE INFO

*Keywords:*
Late Miocene
Marine gateways
Mediterranean-Atlantic exchange
Messinian Salinity Crisis
Palaeogeography
Rif

ABSTRACT

The Rifian Corridor was one of the Mediterranean–Atlantic seaways that progressively restricted and caused the Messinian Salinity Crisis (MSC). Many key questions concerning the controls on the onset, progression and termination of the MSC remain unanswered mainly because the evolution of these seaways is poorly constrained. Uncertainties about the age of restriction and closure of the Rifian Corridor hamper full understanding of the hydrological exchange through the MSC gateways: required connections to sustain transport of salt into the Mediterranean for the primary-lower gypsum and halite stages.

Here we present integrated surface-subsurface palaeogeographic reconstructions of the Rifian Corridor with improved age-control. Information about age and timing of the closure have been derived from high-resolution biostratigraphy, palaeoenvironmental indicators, sediment transport directions, and the analysis of published onshore subsurface (core and seismic) datasets. We applied modern taxonomic concepts to revise the biostratigraphy of the Rifian Corridor and propose astronomically-tuned, minimum-maximum ages for its successions. Finally, we summarise the palaeogeographic evolution in four time slices corresponding to the middle Tortonian (10.57–8.37), late Tortonian (8.37–7.25 Ma), early Messinian (7.25–6.35 Ma), and late Messinian (6.35–5.33 Ma).

Several successions record the closure of the corridor via a continuous marine to continental-lacustrine transition. The youngest dated marine sediments represent a good approximation of the age of seaway closure. The closure of the South Rifian Corridor is constrained to 7.1–6.9 Ma; that of the North Rifian Corridor is more uncertain and ranges from 7.35 to ca. 7 Ma. We conclude that the Rifian Corridor was already closed in the early Messinian and did not contribute to the restriction events that resulted in the MSC. Because the Betic Corridor is also closed by the early Messinian, the modern Gibraltar Straits remain the sole option in the Western Mediterranean as last Messinian seaway that was open during the MSC. Our results imply that the Gibraltar Straits could have been established as the exclusive Mediterranean-Atlantic portal already in the late Miocene, and therefore we suggest that future field and drilling campaigns should target the Alboran Sea and the Gibraltar region to investigate water exchange before and during the Messinian Salinity Crisis and its impact on Atlantic circulation and global climate.

## 1. Introduction

Changes in configuration of the Mediterranean-Atlantic seaways during the Miocene had a crucial impact on the exchange of heat, salt and nutrients. This reconfiguration paved the way for the extreme salinity fluctuations occurring in the Mediterranean during the late Miocene (e.g., (Flecker et al., 2015; Jolivet et al., 2006)). The palaeogeographic evolution of the late Miocene, Mediterranean-Atlantic seaways (Fig. 1) became particularly relevant as the chronology of the Messinian Salinity Crisis (MSC) became better constrained (5.97–5.33 Ma; (Krijgsman et al., 1999a; Manzi et al., 2013)), revealing stepwise palaeoenvironmental changes in pre-evaporite (Kouwenhoven et al., 2003; Kouwenhoven et al., 2006) and evaporite-bearing (Lugli et al., 2010; Roveri et al., 2008) successions. Models revealed that at

* Corresponding author.
*E-mail address:* wcap41@gmail.com (W. Capella).

https://doi.org/10.1016/j.earscirev.2018.02.017
Received 23 April 2017; Received in revised form 4 February 2018; Accepted 12 February 2018
Available online 22 February 2018
0012-8252/ 

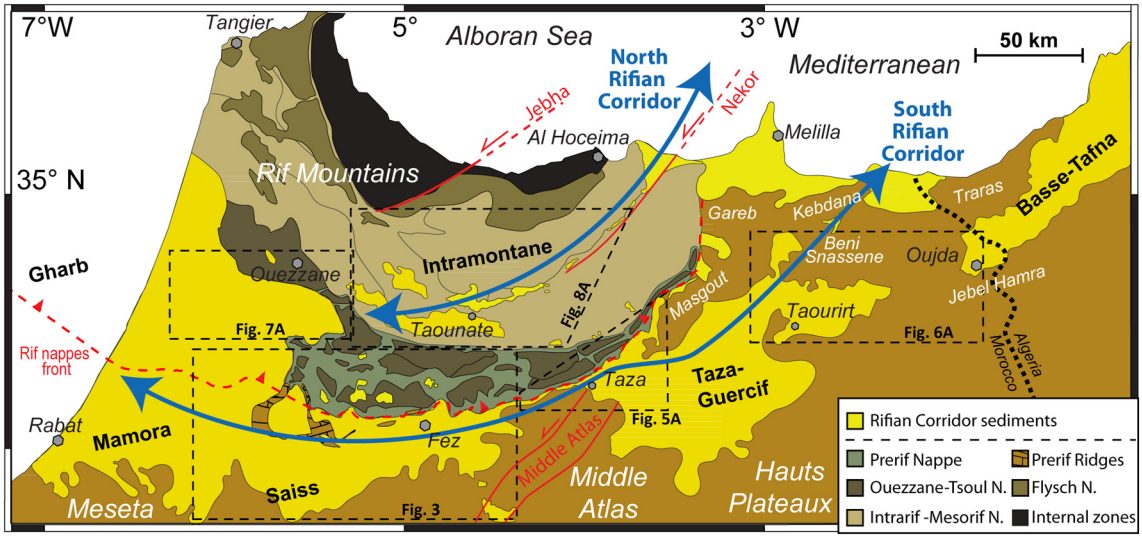


**Fig. 1.** Simplified geological map with the tectonic units composing the Rif fold and thrust belt. The Rifian Corridor sediments are upper Tortonian and lower Messinian deposits locally covered by Quaternary cover; they represent the approximate extension of the Late Miocene seaway. Tectonic units modified from (Capella et al., 2017b; Chalouan et al., 2008).

least one seaway to the Atlantic remained open until ~5.55 Ma to deliver the sea-water necessary for the deposition of km-thick evaporites on the Mediterranean seafloor during the MSC (Krijgsman and Meijer, 2008; Roveri et al., 2014). This seaway is currently unfound (Achalhi et al., 2016; Hüsing et al., 2010).

The MSC occurred at the peak of a process of isolation of the Mediterranean from the open ocean that started with the closure of the Tethys at about 30–35 Ma (Jolivet et al., 2006). With the final closure of the Eastern Tethys gateway around 11 Ma (Hüsing et al., 2009b; Rögl, 1999), the region of Gibraltar became the sole connection between the Mediterranean and the world ocean. Restriction of the Betic and Rifian corridors (Fig. 1), the two portals of this ancestral Gibraltar connection, is thought to have triggered the MSC, which was ended by the re-establishment of fully marine conditions at 5.33 Ma (e.g., (Flecker et al., 2015)). Temporary closure of these two portals or other areas of the Western Mediterranean during the Messinian created a land bridge that allowed African and Iberian mammals to exchange already at ~6.2 Ma (Agustí et al., 2006), and, subsequently, caused the Mediterranean sea-level to drop temporarily (Krijgsman and Meijer, 2008; Roveri et al., 2014).

The role of the Rifian Corridor's closure in the isolation of the Mediterranean is still debated. The Rifian Corridor is regarded by some as the last open seaway before complete disconnection from the Atlantic (e.g., (Martín et al., 2001)). However, stratigraphic evidence only supports that the corridor opened around 8–9 Ma, and closed between 6.7 and 6.0 Ma (Achalhi et al., 2016; Krijgsman et al., 1999b) so the presence of an open seaway through Morocco between 6.7 and 5.55 Ma remains unclear (Achalhi et al., 2016; Flecker et al., 2015; Krijgsman et al., 1999b; Simon and Meijer, 2015).

To improve our understanding of the palaeogeographic evolution of the seaway, and to test the Rifian Corridor as potential last Mediterranean-Atlantic seaway, we reconstructed the ancient seaway environments by studying its preserved sediments. Early works (e.g., (Suter, 1980; Wernli, 1988)) provided the framework for the study of the Rifian Corridor sedimentary domains; however, the youngest seaway sediments are often grouped together as an undifferentiated Tortonian-Messinian unit, with an age range of 7.8–5.3 Ma (see Sections 2 and 3.2).

Besides uncertainties in the dating methods, palaeogeographic reconstructions are mostly dictated by the preservation pattern of the sediments. The map in Fig. 1 (modified after (Wernli, 1988)) shows the extension of the Rifian Corridor sediments, which have been used to locate the ancient seaway, commonly divided in its northern and southern arms (e.g., (Achalhi et al., 2016; Duggen et al., 2003; Flecker et al., 2015; Martín et al., 2001; Martín et al., 2009)). It is unclear how much of these seaway patterns (Fig. 1) reflect the original geometry of the seaway and how much is a function of the preservation of the sediments after uplift and erosion (Flecker et al., 2015). Higher resolution structural data have become recently available based on outcrop and subsurface observations ((Capella et al., 2017b); Tulbure et al., 2017), which may form the base of more quantitative reconstructions.

It is crucial to base the reconstructions on the tectono-sedimentary evolution of the marine gateway, which is only possible if age and palaeo-environments are better constrained. Therefore, the aims of this new palaeogeographic reconstruction of the Rifian Corridor are to: (i) apply a revised and enhanced planktic foraminiferal stratigraphy to provide a higher resolution correlation and dating of the late Miocene sediments in the Rifian Corridor and hence constrain the timing of its evolution; (ii) estimate the evolution of the palaeo-depth and environment of deposition of the sedimentary successions with changes in benthic foraminiferal assemblages; (iii) use detailed sedimentology analysis to assess the likely dimensions and geometry of the connections and evaluate their similarity to the current two-strand preservation model for the corridor; (iv) reconstruct the palaeogeographic evolution of the Mediterranean-Atlantic connection through northern Morocco and asses its implications for the Messinian Salinity Crisis and outflow to the Atlantic.

Basin to basin correlation across the Rifian Corridor is achieved with cross-sections based both on surface and subsurface data; and identification of syn-kinematic deposition driven by tectonic events. We aimed at understanding the relationship between different basins, including their possible links based on the geometry of strata at their margins. Based on this relationship we can infer whether the area reflects the true palaeo-basin margin or simply an area of localised uplift which post-dates deposition (e.g., (Bertotti et al., 2006)).

Our results are then integrated with existing literature (e.g., (Achalhi et al., 2016; Barhoun and Bachiri Taoufiq, 2008; Capella et al., 2017a; Dayja et al., 2005; Dayja, 2002; Feinberg, 1986; Feinberg, 1978; Hilgen et al., 2000a; Krijgsman et al., 1999b; Krijgsman et al., 2004; Samaka et al., 1997; Wernli, 1988); Tulbure et al., 2017) and unpublished data acquired for petroleum exploration (e.g., (SCP/ERICO report, 1991; SOQUIP report, 1990)), to create four maps of the Rifian Corridor illustrating its late Miocene evolution. These maps provide constraints that have implications both for the onset and development of the Messinian Salinity Crisis in the Mediterranean (Flecker et al., 2015), for the initiation of Mediterranean overflow into the Atlantic

(Capella et al., 2017a) and its contribution to the transition from a global greenhouse to icehouse environment (Herbert et al., 2016; Potter and Szatmari, 2009). Since these palaeo-gateways preserve fossil imprints of the oceanic currents representative of exchange between the Mediterranean Sea and the Atlantic, these palaeogeographic reconstructions provide insights into changes in gateway geometry which can significantly alter the pattern of Mediterranean hydrology and ocean circulation and hence heat transport and climate.

## 2. Palaeogeography and geological background

Feinberg (Feinberg, 1986; Feinberg, 1978) and Wernli (Wernli, 1988) pioneered the palaeogeographic reconstructions of the Rifian Corridor that are still widely used today (e.g., (Benson et al., 1991; Duggen et al., 2003; Martín et al., 2001; Martín et al., 2009; Santisteban and Taberner, 1983)). These early reconstructions identified a post-orogenic marine sedimentary cover that unconformably overlies the Rif thrust systems (*Miocène post-nappe*), therefore indicating a marine passage where water flowed over a submerged orogenic foreland (Fig. 1).

The main elements of the Rif fold-and-thrust belt are the internal zones (Alboran domain), and the external zones composed of Flysch units, Intrarif, Mesorif and Prerif, which comprise marine successions deposited between Mesozoic to Miocene on either the Ligurian-Maghrebian ocean floor or the Maghrebian (African) margin itself (see (Chalouan et al., 2008; Platt et al., 2003), for comprehensive overviews). The Rif belt is the southern branch of the Betic-Rif arc (Fig. 1). The formation of this orogen was associated with rapid, Miocene retreat of the Gibraltar slab and collision of the Alboran microplate with the African-Iberian margins (e.g., (Morley, 1993; Van Hinsbergen et al., 2014; Vergés and Fernàndez, 2012)). The thin-skinned, contractional deformation continued until emplacement of the outermost thrusted units in the late Tortonian, at around 8 Ma (Do Couto et al., 2016; Van Hinsbergen et al., 2014).

The main basins in which the Rifian Corridor, post 8 Ma sediments are preserved are the Gharb, Saiss and Taza-Guercif basins to the south, which are continuously connected forming the South Rifian Corridor ((Dayja et al., 2005; Krijgsman et al., 1999b); Fig. 1); and the less connected Had Kourt, Taounate, Dhar Souk depocentres further north, which seem to connect to the Arbaa Taourirt and Boudinar basins near the Mediterranean coast (Fig. 1; (Achalhi et al., 2016); Tulbure et al., 2017). The Gharb Basin was the western mouth of both strands of the Rifian Corridor and, following gateway closure, continued to record deposition as an Atlantic embayment (e.g., (Cirac, 1987; Ivanovic et al., 2013; Wernli, 1988)).

Other available palaeogeographic reconstructions contain significant information in terms of stratigraphy and geometry, but are affected by similar uncertainties and cover only parts of the Rifian Corridor, such as the Saiss (e.g., (Charrière and Saint-Martín, 1989; Saint-Martín and Charrière, 1989)) or Gharb Basin (Cirac, 1987; Rabaté, 1965; Rabaté, 1971; SCP/ERICO report, 1991; SOQUIP report, 1990; Tachet des Combes, 1967; Tachet des Combes, 1971), and therefore do not provide a complete picture of the entire corridor. We referred to some of these local reconstructions to compile the subsurface transects and the final maps.

The total thickness of the post-orogenic cover reaches up to 2500 m, both in wedge-top and foredeep settings (e.g., (Flinch, 1993; Samaka et al., 1997; Sani et al., 2000; Sani et al., 2007; Wernli, 1988)). This post-orogenic cover mostly consists of siliciclastic, marl-sandstone alternations called the “Blue Marls or Blue Marl Formation” in recent literature (Benson et al., 1991; Hilgen et al., 2000a; Sani et al., 2007), and *Marnes Bleues du Maroc*, or *Néogène post-nappes* in earlier publications (e.g., (Feinberg, 1986; Wernli, 1988)). This clastic succession also includes, at limited locations, the products of carbonate factories. These locations are the Gulf of Skoura (Fig. 3), in the SE part of the Saiss Basin, and the Melilla embayment, on the Mediterranean side of the corridor (Charrière and Saint-Martín, 1989; Saint-Martín and Charrière, 1989; Saint-Martín and Cornée, 1996). Between the Melilla embayment and the Taza-Guercif Basin, the products of coeval volcanic activity are mixed with the siliciclastic seaway deposits (Wernli, 1988).

Although the Rifian Corridor is commonly subdivided into a northern and a southern strand and two distinct Mediterranean-Atlantic connections are envisaged (e.g., (Achalhi et al., 2016; Flecker et al., 2015)), there are several patches of marine Blue Marl Formation that unconformably overlie the intervening Prerif Nappe (Fig. 1) suggesting a wider seaway that may have linked, at times, these two main strands (Capella et al., 2017b). Sedimentary thickness in these areas is limited by comparison to the main depocentres which may either suggest deposition on submarine highs or additional erosion due to subsequent uplift.

### 2.1. Linking the early and middle Miocene to the late Miocene configuration

An earlier and supposedly wider Mediterranean-Atlantic seaway existed from Cretaceous to Middle Miocene as part of the Ligurian-Maghrebian Ocean (e.g., (Do Couto et al., 2016; Jolivet et al., 2006)). Its sedimentary remnants were incorporated in the Rif thrust-systems (Chalouan et al., 2008; Morley, 1988; Morley, 1992) during the orogenic phase that ceased in the late Tortonian creating the Betic-Rif arc (Crespo-Blanc et al., 2016; Do Couto et al., 2016; Jolivet et al., 2006; Van Hinsbergen et al., 2014; Vergés and Fernàndez, 2012). In Morocco, several lines of evidence suggest that the last pulse of Miocene nappe-stacking occurred during the middle-late Tortonian in a submerged foreland, which gradually shifted south to south-westward as a result of flexure caused by the Prerif (=*Prerifaine*) Nappe emplacement, the frontal part of the orogenic wedge (e.g., (Capella et al., 2017b; Feinberg, 1986; Flinch, 1993; Gomez et al., 2000; Sani et al., 2007; Suter, 1980; Zouhri et al., 2002)). The submarine character of this event is deduced from the presence of Middle Miocene planktic foraminiferal assemblages found in mudstones that are mixed with the Prerif Nappe (Feinberg, 1986; Leblanc, 1979). As a result of this orogenic phase, the sediments of the Early-Middle Miocene seaway, where preserved, formed the substrate of the late Miocene Rifian Corridor as part of the nappes or shallow marine clastic facies in foredeep position ((Sani et al., 2007); Fig. 2B).

The seaway reached the present areas of the Southern Gharb, Saiss and Taza-Guercif basins as a consequence of this flexural bending around 8 Ma (Bernini et al., 2000; Gelati et al., 2000; Gomez et al., 2000; Sani et al., 2007; Zouhri et al., 2002), which is the age of the onset of undeformed, post-orogenic sedimentation in most locations of the Rifian Corridor ((Achalhi et al., 2016; Dayja et al., 2005; Flecker et al., 2015; Hilgen et al., 2000a; Krijgsman et al., 1999b); Fig. 2A–B). From 8 Ma onwards the configuration of the Rif orogen did not change substantially (e.g., (Jolivet et al., 2006; Krijgsman and Garcés, 2004; Van Hinsbergen et al., 2014)) since clastic marine sediments were deposited both above the wedge-top basins (e.g., Taounate and the intramontane basins to the north-east of it; (Samaka et al., 1997; Wernli, 1988); Fig. 1) and in the foreland basins to the south (the Gharb, Saiss, and Taza-Guercif basins; (Dayja et al., 2005; Krijgsman et al., 1999b; Sani et al., 2007; Wernli, 1988); Fig. 1).

## 3. Methods

The data presented in this study is derived from field observations (along sections and regional) specifically obtained for this study, and subsurface data (seismic profiles and boreholes) integrated from literature. Surface data was obtained during field campaigns carried out in December 2012; February and April 2013; January/February and September/October 2014; May 2015 and January 2016. These data were correlated with available literature data on the subsurface architecture of the multiple Rifian Corridor basins (e.g., (Dayja et al., 2005; Gomez et al., 2000; Samaka et al., 1997; Sani et al., 2000; Sani et al.,

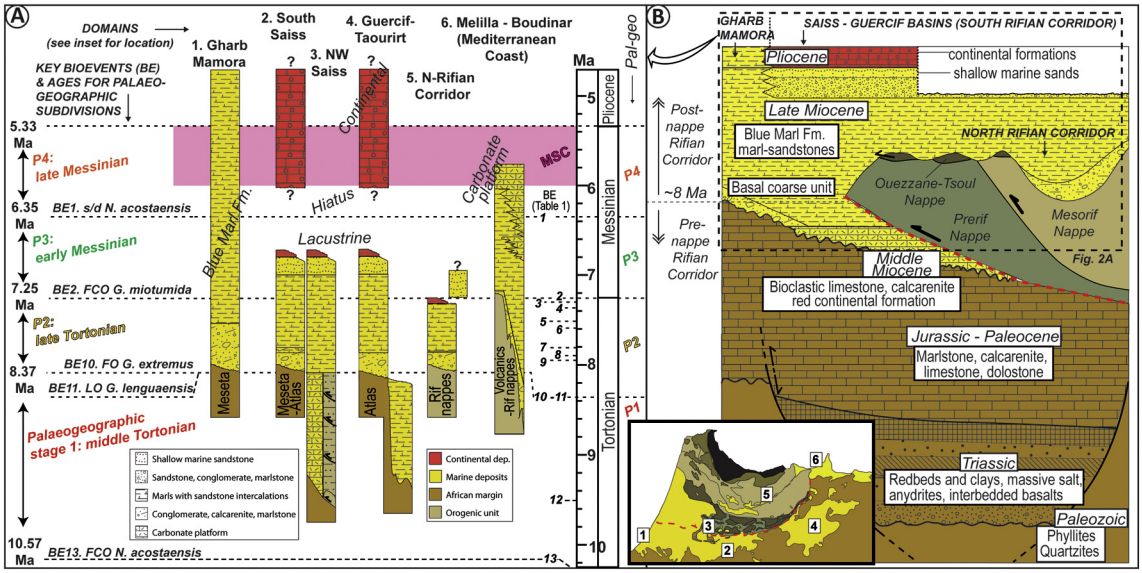


**Fig. 2.** (A) Synthesis of the stratigraphic domains of the Rifian Corridor from east to west (modified after van Assen et al., 2006) and biostratigraphic framework used in the present study to refine the stratigraphy of the Upper Miocene Rifian Corridor. Bioevents written in full are those marking boundaries between the four palaeogeographic subdivisions; other bioevents and relative references are shown in Table 1. The time span of the Messinian Salinity Crisis (MSC) is shown in pink colour. (B) Stratigraphic column and tectonogram illustrating the relationship between litho-stratigraphy and tectonic in the foreland of the Rif orogen (compiled from (Capella et al., 2017b; Sani et al., 2007), and the results of the present study). (For interpretation of the references to colour in this figure legend, the reader is referred to the web version of this article.)

2007)), to which we refer specifically in the figures showing the resulting cross-sections, and internal reports on the subsurface of the Gharb-Saiss basin (SCP/ERICO report, 1991; SOQUIP report, 1990) Table 2.

### 3.1. Sections and palaeogeography

Forty-three field sites and six boreholes were studied across the area of the Rifian Corridor (Fig. 1 and relative insets). Given the strong relationship between sedimentation and the mechanics and development of orogenic forelands (e.g., (Mutti et al., 2003)), collection of data was oriented in such a way to detect (i) the onset marine transgression in foredeep and associated wedge-top basins, (ii) the stages of foreland basin subsidence, and (iii) the regressive stage of basin fill associated with the transition to continental deposits after the cessation of thrust movements (e.g., (Mutti et al., 2003; Roure, 2008)). In the Rifian Corridor, the Tortonian-Quaternary evolution of the foreland basins was characterised by in initial phase of low-angle thrusting associated with the formation of the foredeep and segmented wedge-top basins, followed by a regional transgression and, ultimately, by a period of thick-skinned, out-of-sequence thrusting that has induced significant uplift, likely associated with the regressive stage of complete basin fill (Capella et al., 2017b).

Our first priority was then to find continuous sections that record the stages of evolution of the late Miocene seaway. These few continuous sections are mostly limited to the Taza-Guercif (Zobzit–Koudiat Zarga; (Krijgsman et al., 1999b)), Saiss (Moulay Yacoub and East Fes; (Capella et al., 2017a; Wernli, 1988), respectively), and Taounate basins (Wernli, 1988). Since most of the surface sections are discontinuous and the successions poorly exposed, we integrated the information from the few, continuous sections with the much more common limited exposures present across the area of the Rifian Corridor in key palaeogeographic positions (Fig. 1). We dated the marine sediments based on the presence or absence of key planktonic foraminifera (Fig. 2A and Table 1), extracted information on environment and palaeo-depth of deposition based on benthic assemblages, and, where possible, inferred direction of palaeoflow based on the measurement of sedimentary structures in sandstones and conglomerates (see also Methods in (Capella et al., 2018)). Field sections and relative information aboutage and palaeo-water depth of deposition are summarised.

In addition, two longitudinal and four transversal cross-sections have been constructed to depict the subsurface geometry of the Rifian Corridor. These reconstructions rely on unpublished reports for oil-exploration (e.g., (SCP/ERICO report, 1991; SOQUIP report, 1990)), cross-sections in regional geological maps (e.g., (Leblanc, 1978a; Leblanc, 1978b; Vidal, 1979a; Vidal, 1979b)) and published seismic data (e.g., (Capella et al., 2017b; Gomez et al., 2000; Samaka et al., 1997; Sani et al., 2000; Sani et al., 2007); Tulbure et al., 2017).

### 3.2. Age and palaeodepth estimation based on planktic and benthic foraminifera

To establish an improved age model and determine the basin evolution of the Rifian Corridor we performed biostratigraphic analysis on many field sections. To cover the vast study area we made use, for some of the sections, of the sets of samples collected for the regional geological maps (Wernli, 1988) and stored at the Ministry of Geology in Rabat. New samples have been collected in key sections (Fig. 1 and relative insets). A semi-quantitative analysis of the planktonic foraminiferal marker species was carried out on the $> 150$ μm size fraction of the washed residue.

Wernli (Wernli, 1988) analysed surface and subsurface data over a vast area of the Rifian Corridor and, although the results are critical for understanding palaeogeography and implications for basins connectivity, his biostratigraphic schemes could not be linked accurately to absolute ages because of missing high-resolution biostratigraphy at that time (see also Methods in Tulbure et al., 2017 for an extensive overview). As a result, large part of the gateway sediments are commonly assigned to an undifferentiated Tortonian-Messinian zone. We have therefore applied the high-resolution astronomically calibrated planktonic foraminiferal biochronology for the Mediterranean and the Atlantic side of the Mediterranean (Table 1). Astronomical calibration of the Oued Akrech and Ain el Beida sections located on the Atlantic side of Morocco (Fig. 1) showed that these events have exactly the same age as in the Mediterranean (Hilgen et al., 2000a; Krijgsman et al., 2004).

Table 1 shows the modern astrobiostratigraphic framework that allowed us to refine the age of the Upper Miocene sediments, and Fig. 2

**Table 1**
Main bioevents used to date the Rifian Corridor sediments. References are for the astronomically calibrated ages in the Mediterranean region and its Atlantic side.

| Event no. (Fig. 2) | Planktonic Foraminifer bioevents | Age (Ma) | Atlantic | Mediterranean |
|---|---|---|---|---|
| 1 | Sinistral to dextral coiling change (S/D) of *Neogloboquadrina acostaensis* | 6.35 | (Sierro et al., 1993) | (Hilgen and Krijgsman, 1999); (Sierro et al., 2001); (Lourens et al., 2004) |
| 2 | Replacement of *Globorotalia menardii* 5 by *Globorotalia miotumida* group | 7.25 | (Sierro, 1985); (Sierro et al., 1993); (Hilgen et al., 2000a) | (Sierro et al., 2001); (Lourens et al., 2004) |
| 3 | S/D coiling change of *Globorotalia scitula* | 7.28 | (Sierro, 1985); (Sierro et al., 1993); (Hilgen et al., 2000a); (Lourens et al., 2004) | (Sierro et al., 1993); (Lourens et al., 2004) |
| 4 | First Common Occurrence (FCO) of *G. menardii* 5 | 7.35 | (Sierro, 1985); (Sierro et al., 1993); (Hilgen et al., 2000a); (Lourens et al., 2004) | (Krijgsman et al., 1995); (Hilgen et al., 1995); (Lourens et al., 2004) |
| 5 | Last Common Occurrence (LCO) *Globorotalia menardii* 4 | 7.51 | (Sierro, 1985); (Sierro et al., 1993); (Hilgen et al., 2000a); (Lourens et al., 2004) | (Krijgsman et al., 1995); (Hilgen et al., 1995); (Lourens et al., 2004) |
| 6 | (Dextral to sinistral (D/S)) coiling change of *G. scitula* group | 7.58 | | (Krijgsman et al., 1997); (Lourens et al., 2004) |
| 7 | First Occurrence (FO) of *Globorotalia suterae* | 7.8 | | (Sprovieri et al., 1999) |
| 8 | Lowest Common Occurrence (lro) of *Sphaeroidinellopsis seminulina* | 7.92 | | (Krijgsman et al., 1995); (Hilgen et al., 1995); (Lourens et al., 2004); (Hüsing et al., 2009a) |
| 9 | Onset dominant sinistral Neoglobquadrinids | 7.92–8 Ma | | (Krijgsman et al., 1995); (Hilgen et al., 1995) |
| 10 | FO of *Globigerinoides obliquus extremus* (Mediterranean) | 8.37 | Tropical Atlantic: 8.93 Ma (Lourens et al., 2004) | (Sprovieri et al., 1999) |
| 11 | Last Occurrence (LO) of *Globorotalia lenguaensis* (Mediterranean) | ~8.37 | Tropical Atlantic: 8.97 Ma (Turco et al., 2002) | (Foresi et al., 2002); F. Lirer, pers. comm. |
| 12 | Highest Regular Occurrence (hro) *N. acostaensis* | 9.51 | | (Krijgsman et al., 1995); (Hilgen et al., 1995); (Lourens et al., 2004) |
| 13 | FRO *N. acostaensis* | 10.57 | | (Hilgen et al., 2000a; Hilgen et al., 2000b); (Lourens et al., 2004) |

depicts the distribution of the key bioevents across the domains of the Rifian Corridor. Based on the tectonic evolution of the area, we selected four time intervals to make our palaeogeographic reconstructions of the Rifian Corridor: 1) the middle Tortonian; 2) the late Tortonian; 3) the early Messinian and 4) the late Messinian. Each subdivision in the palaeogeographic reconstruction is derived from a cluster of sediments in the field that share the same biostratigraphic assemblage. These biostratigraphy-based subdivisions also share the same geological stage of foreland-basins mentioned in Section 3.1 (i.e. (i) foredeep inception, (ii) infilling, and (iii) closure). The four chronologic subdivisions are based on the age intervals encased in the following bioevents (see Table 1 for respective references):

#### 3.2.1. Middle Tortonian

The lower boundary of this age interval is represented by event 13, the First Common Occurrence (FCO) of *Neogloboquadrina acostaensis* at 10.57 Ma. The upper boundary is set by events 11 and 10. Event 11 is the Last Occurrence (LO) of *Globorotalia lenguaensis*, which occurs at 8.37 Ma in the Mediterranean domain, but can occur earlier in the tropical Atlantic (8.97 Ma). Event 10 is set at 8.37 Ma by the First Occurrence (FO) of *Globigerinoides extremus* in the Mediterranean domain, and also occurs earlier in the tropical Atlantic (8.93 Ma). This age interval is much less-constrained than those following event 10, partly due to the last pulse of thin-skinned tectonics which led to substantial basin reconfiguration before 8 Ma (e.g., (Crespo-Blanc et al., 2016; Morley, 1987; Morley, 1988; Morley, 1992)). Consequently the middle Tortonian palaeogeographic map will represent an approximation of the pre-nappe configuration (including partly the Middle Miocene) rather than an exact reconstruction of palaeoenvironments between 10.57 and 8.37 Ma.

#### 3.2.2. Late Tortonian

This age interval post-dates the FO of *G. extremus* (event 10). The upper boundary is set by the replacement of the *Globorotalia menardii* group by the *Globorotalia miotumida* group at 7.25 Ma (event 2;Table 1). Besides *G. extremus,* other species or assemblages of species mark ages that are part of this interval. Examples of these typical species are the following: *Sphaeroidinellopsis seminulina* (event 8); *Globorotalia suterae* in the Mediterranean domain (event 7); *Globorotalia menardii 4* (event 5); *Globorotalia menardii 5* (event 4); predominantly sinistral *N. acostaensis* (event 9; Table 1).

#### 3.2.3. Early Messinian

This age interval post-dates event 2, the FCO of *Globorotalia miotumida* (7.25 Ma) and pre-dates the coiling change of *N. acostaensis* from predominantly sinistral to dextral forms occurring at 6.35 Ma (event 1; Table 1).

#### 3.2.4. Late Messinian

This age interval spans between event 1 and the Mio-Pliocene boundary at 5.33 Ma (Lourens et al., 2004). Sediments belonging to this biochronostratigraphic zone are only identified on the Atlantic side (e.g., Rabat sections; (Krijgsman et al., 2004)). More internal parts of the corridor record continental deposition before event 1 (6.35 Ma) and therefore the dominant palaeoenvironment for the late Messinian is inferred to be continental, possibly lacustrine or alluvial. Because dating of the continental unit remains poorly constrained, our biostratigraphic framework stops at the continental transition.

In addition, we studied the benthic assemblages from the washed residues to estimate depth and palaeo-environment at time of deposition. Depth-distribution of groups of benthic foraminifera known from literature can be applied (e.g., (Pérez-Asensio et al., 2012; Schönfeld, 1997; Schönfeld, 2002)). Although the slope profiles of the Rifian Corridor are likely to have been different from the continental margins on which these estimates are based, the distinction between shelf and slope type faunas is indicative of a shallower or deeper setting,

**Table 2**
Age and palaeoenvironment of deposition of the outcrops and wells used to reconstruct the Rifian Corridor palaeogeography.

| | Site and log number | Site name | Well_Outcrop | Previous works | Max–min age in my (events in Table 1) | Palaeoenvironments | Max–min depth (m) | Palaeogeographic stage |
|---|---|---|---|---|---|---|---|---|
| Prerif Ridges, Saiss Basin and associated outcrops (Figs. 3 and 4) See (Capella et al., 2018) for details | 1 | Bab Tisra | Outcrop | (SCP/ERICO report, 1991) (Roldán et al., 2014) | M1, 2: Miocene undifferentiated (SCP/ERICO report, 1991) M3 (this study): 8.37 (10)–7.92 (9) | M1, 2: coastal marine to inner shelf (SCP/ERICO report, 1991) M3: transgressive, deepening–upward sequence, from coastal marine to upper bathyal | M1, 2: 0–50 M3: 0–50 to 200–300 | M1, 2: P1? M3: P2 |
| | 2 | Ben Allou | Outcrop | (Capella et al., 2017a) | 7.80 (7)–7.51 (5) | Outer shelf to upper bathyal | 150–300 | P2 |
| | 3 | Moulay Yacoub | Outcrop | (SCP/ERICO report, 1991) (Wernli, 1988) | 7.92 (8)–6.35 (1) | Upper bathyal, shallowing upward to middle shelf | 300–500 to 50–100 | P2–P3 |
| | 4 | East Fes<br><br>Subsections:<br>Sidi Harazem (SH)<br>El Adergha (EA)<br>Ain Kansera (AK) | Outcrop | (Wernli, 1988); (Capella et al., 2017a) | 7.92 (8)–7.25 (2) | Upper bathyal shallowing upward to outer shelf (SH + EA, Fig. 4); a laterally equivalent sequence shallows upward from inner shelf to coastal marine (AK) | 240–400 (SH) 150–300 (EA) 50–100 to 15–50 (AK) | P2 |
| | 5 | Bir Tam Tam | Outcrop | – | 7.58 (6)–7.35 (4) | Outer shelf/upper bathyal | 150–300 | P2 |
| | 6 | Boudhilet | Outcrop | – | 9.51 (12)–8.37 (10) | Outer shelf/upper bathyal | 150–300 | P1 |
| | 7 | Karia ba Mohammed | Outcrop | – | Middle Miocene und. | Outer shelf/upper bathyal or deeper | ? | P1? |
| | 8 | Jebel Lemda | Outcrop | – | 7.80 (7)–7.51 (5) | Shallowing upward from upper bathyal to shelf/slope transition | 400–500 to 150–250 | P2 |
| | 9 | Beni Ammar | Outcrop | – | 7.92 (8)–7.51 (5) | Middle bathyal | 600–800 | P2 |
| | 10 | Jenanat | Outcrop | (Dayja, 2002); (Dayja et al., 2005) | 7.80 (7)–7.25 (2) (Dayja et al., 2005) | Deepening upward sequence from inner shelf depth to upper bathyal (Dayja, 2002) | 30–50 to 300–400 | P2 |
| | 11 | Madhouma | Outcrop | (Wernli, 1988); Barbieri and Ori, 2000 | 7.25 (2)–6.35 (1) | Shallowing upward sequence from middle shelf to continental | 50–150 to 0 | P3 |
| | 12 | Ain Lorma | Outcrop | (Wernli, 1988) | 7.25 (2)–6.35 (1) | Shallowing upward sequence from upper bathyal to shelf; from inner shelf to continental | 200–400 to 0 | P3 |
| | 13 | Douar Zaouia S. | Outcrop | – | 7.25 (2)–6.35 (1) | Inner shelf | 0–50 | P3 |
| | 14 | Haricha | Outcrop | (SCP/ERICO report, 1991); (Capella et al., 2017a) | 7.25 (2)–6.35 (1) | Shelf break/upper bathyal | 150–250 | P3 |
| | 15 | Gulf of Skoura | Outcrop | (Wernli, 1988); (Charrière and Saint-Martín, 1989); (Saint-Martín and Charrière, 1989) | Late Tortonian/early Messinian? (Wernli, 1988) | Inner/middle shelf | 0–100 | P2–P3 |
| | 16 | Jebel Trhat | Outcrop | (Wernli, 1988) | 7.92 (8)–7.25 (2) | – | – | P2 |
| | 17 | Douyet | Well | (Dayja, 2002); (Dayja et al., 2005); (Barhoun and Bachiri Taoufiq, 2008) | ~8–7.12 (Dayja et al., 2005) | – | – | P2–P3 |
| | 18 | Koudiat el Griouine | Outcrop | (Wernli, 1988) | – | – | – | – |
| Taza area (Fig. 5) See (Capella et al., 2018) for details | 19 | Col Touahar | Outcrop | – | ~8–7.51 (5) | deepening-upward sequence from inner to outer shelf | 0–50 to 100–200 | P2 |
| | 20 | Bouhlou | Outcrop | – | ~8–7.51 (5) | shelf und. | – | P2 |
| | 21 | Taza | Outcrop | – | 8.37 (10)–7.51 (5) | Middle/outer shelf | 50–200 | P2 |
| | 22 | Ouled Bourima | Outcrop | – | 7.80 (7)–7.51 (5) | Upper bathyal (truncated by erosional unconformity and capped by continental deposits at the top) | 300–500 | P2 |
| | 23 | Ain Zohra | Outcrop | – | 8.37 (10)–7.51 (5) | Shelf break/upper bathyal | 200–300 | P2 |
| | 24 | AKL–101 | Well | (Gomez et al., 2000); (Barhoun, 2000) | uppermost 300 m: 7.58 (6)–7.51 Ma (5) (Barhoun, 2000) | – | – | P2 |

(*continued on next page*)

**Table 2** (*continued*)

| | Site and log number | Site name | Well_Outcrop | Previous works | Max–min age in my (events in Table 1) | Palaeoenvironments | Max–min depth (m) | Palaeogeographic stage |
|---|---|---|---|---|---|---|---|---|
| Taourirt–Oujda depocentres (Fig. 6) See (Capella et al., 2018) for details | 25 | Hassi Berkane | Outcrop | – | 10.57 (13)–8.37 (10) | Upper bathyal | 200–600 | P1 |
| | 26 | Hassi Berkane | Outcrop | – | 10.57 (13)–8.37 (10) | Upper bathyal | 200–600 | P1 |
| | 27 | Hassi Berkane | Outcrop | – | no foraminifera | Continental | – | P2? |
| | 28 | Hassi Berkane | Outcrop | – | no foraminifera | Continental | – | P2? |
| | 29 | Taourirt | Outcrop | – | 7.80 (7)–7.35 (4) | Outer shelf | 100–200 | P2 |
| | 30 | Taourirt | Outcrop | – | no foraminifera | Lagoonal/continental | – | P2 |
| | 31 | El Aioun | Well | (Wernli, 1988) | – | Continental | – | P2? |
| | 32 | Beni Oulik | Well | (Wernli, 1988) | 7.80 (7)–7.25 (2) (Wernli, 1988) | Inner/middle shelf | 0–100 | P2 |
| | 33 | Angad | Well | (Wernli, 1988) | 7.80 (7)–7.25 (2) (Wernli, 1988) | – | – | P2 |
| Northern Gharb (Fig. 7) See (Capella et al., 2018) for details | 34 | Jebel Dahl | Outcrop | (SCP/ERICO report, 1991) | 7.25 (2)–6.35 (1) | Outer shelf/upper bathyal | 100–300 | P3 |
| | 35 | NRT–2 | Well | (Barhoun, 2000) | 7.25 (2)–6.35 (1) (Barhoun, 2000) | – | – | P3 |
| | 36 | Jebel Bibane | Outcrop | (SCP/ERICO report, 1991) | 7.25 (2)–6.35 (1) | Outer shelf/upper bathyal | 100–300 | P3 |
| | 37 | El Sila | Outcrop | – | older than 7.25 (2) | Shelf und. | 0–200 | P2? |
| | 38 | Moulay Abdelkrim | Outcrop | (SCP/ERICO report, 1991) | older than 7.25 (2) | Shelf und. | 0–200 | P2? |
| | 39 | Mzrefroun | Outcrop | – | older than 7.25 (2) | Inner/middle shelf | 0–100 | P2? |
| North Rifian Corridor (Fig. 8) See Tulbure et al., 2017 for details | 40 | Sfasef | Outcrop | Tulbure et al., 2017 | 7.58 (6)–7.35 (4) | Outer shelf/upper bathyal | 150–300 | P2 |
| | 41 | Taounate | Outcrop | (Wernli, 1988) Tulbure et al., 2017 | 7.92 (8)–7.51 (5) | Mid-outer shelf | 100–250 | P2 |
| | 42 | Bouhaddi | Outcrop | Tulbure et al., 2017 | 7.58 (6)–7.35 (4) | Middle shelf | 100–150 | P2 |
| | 43 | Bouhaddi | Outcrop | Tulbure et al., 2017 | 7.58 (6)–7.35 (4) | Middle shelf | 100–150 | P2 |
| | 44 | Dhar Souk | Outcrop | (Wernli, 1988); Tulbure et al., 2017 | 7.92 (8)–7.35 (4) | Shallowing upwards from Mid-outer shelf to middle shelf | 100–250 to 100–150 | P2 |
| | 45 | Sidi Ali Ben Daoud | Outcrop | (Wernli, 1988); Tulbure et al., 2017 | 7.92 (8)–7.51 (5) | Middle shelf | 50–150 | P2 |
| | 46 | Boured | Outcrop | (Wernli, 1988); Tulbure et al., 2017 | 7.92 (8)–7.51 (5) | Middle shelf | 50–150 | P2 |
| | 47 | Arbaa Taourirt | Outcrop | (Achalhi et al., 2016) Tulbure et al., 2017 | 7.80 (7)–7.35 (4) | Shallowing upward from Outer shelf /upper bathyal to mid-outer shelf | 150–300 to 100–200 | P2 |
| | 48 | Arbaa Taourirt (Tarhzout Ntassa) | Outcrop | Tulbure et al., 2017 | 7.80 (7)–7.51 (5) | Outer shelf/upper bathyal | 150–300 | P2 |
| | 49 | Msila | Outcrop | Tulbure et al., 2017 | Early to Middle Miocene | – | – | – |

respectively (see also the methodology part in (Capella et al., 2017a), for an overview of the factors influencing benthic assemblages in the Rifian Corridor). In assemblages where both shelf- and slope-type species are present, we considered that the shallow marine species (such as discorbids, *Ammonia*, *Elphidium* and *Rosalina* species: e.g., (Rogerson et al., 2011)) were transported downslope. Unlike the planktic foraminifera that allow highly accurate biostratigraphy, many species of benthic foraminifera remained morphologically similar throughout the middle-late Miocene. Therefore, in each case we tested the planktic assemblage for possible reworking from older Miocene units.

## 4. Basin lithofacies, stratigraphy and palaeoenvironments

We have subdivided the Rifian Corridor into five individual regions as follows. Three representing the southern domain: i) Prerif Ridges and Saiss Basin, ii) Taza, iii) Taourirt-Oujda; the other two characterising the northern strand: iv) Northern Gharb and v) Intramontane basins (Fig. 1). For each region we present a summary of the main basin evolution trends that are based on lithofacies and inferred palaeoenvironment analyses from a total of 50 sections and sites. Details of each individual section, including microfaunal assemblages, sedimentary facies, field pictures, are presented in an associated Data in Brief article (Capella et al., 2018), excluding the Intramontane Basins (Section 4.5) whose field data were published separately (Tulbure et al., 2017) following a comparable format.

### 4.1. Prerif Ridges and Saiss Basin (Fig. 3)

The Saiss Basin contains Middle Miocene to Messinian foreland deposits. Upper Miocene sections in this area unconformably overlie either the frontal part of the orogenic wedge or the African margin (Fig. 4). The onset of foreland clastic sedimentation started synchronously in the late Tortonian, the maximum age of the individual sections being identified between 8.37 and 7.80 Ma (Table 1; event 10 and 7, respectively). However, a small number of locations records sedimentation in the Middle Miocene (up to middle Tortonian) as shallow, mixed carbonatic platform settings or in wedge-top basins (Bab Tisra, Karia ba Mohammed, Boudhilet; Fig. 4, logs 1, 6, 7, respectively). Only at one location above the orogenic wedge (Haricha, Fig. 4, log 14), foreland sedimentation starts later in the early Messinian, probably due to local structural control (active thrusts) on accommodation space (Capella et al., 2017a).

The key example of upper Tortonian foredeep transgression is Bab Tisra (Fig. 3; point 1). This section is located in the Prerif Ridges area (Fig. 3) and records the transition from Miocene shallow marine lithofacies to deep marine upper Tortonian white marlstones and siltstones (M3 in Fig. 4, log 1). Biostratigraphic analyses dates these marlstones and siltstones at 8.37–8 Ma (Capella et al., 2018). These marlstones overlie bioclastic sandstones and packstones that include reworked clasts from the coastal–marine units below, and reflect a deeper environment with very scarce terrigenous and bioclastic input. The upper Tortonian unit is therefore interpreted as a transgressive, deepening–upward sequence.

This sequence may reflect the gradual flexural loading of the Rif foreland due to the nappe–thrusts reaching the area between 8.37 and 7.92 Ma. Throughout the Miocene, the area of Bab Tisra and the Prerif Ridges (Fig. 3) was probably a marginal embayment corresponding to the southern margin of the Ligurian–Maghrebian Ocean, in which the flysch series was deposited further north (e.g., (Chalouan et al., 2008; Sani et al., 2007)). The advancing thrust systems caused a southward migration of the foreland environments. This process of southward transgression is recorded at the same time (ca. 8 Ma) in the well–studied section located in the marginal areas of the South Rifian Corridor, namely the Rabat, Jenanat, Zobzit sections of the Mamora, Saiss, Taza–Guercif basins, respectively (Dayja et al., 2005; Hilgen et al., 2000a; Krijgsman et al., 1999b).

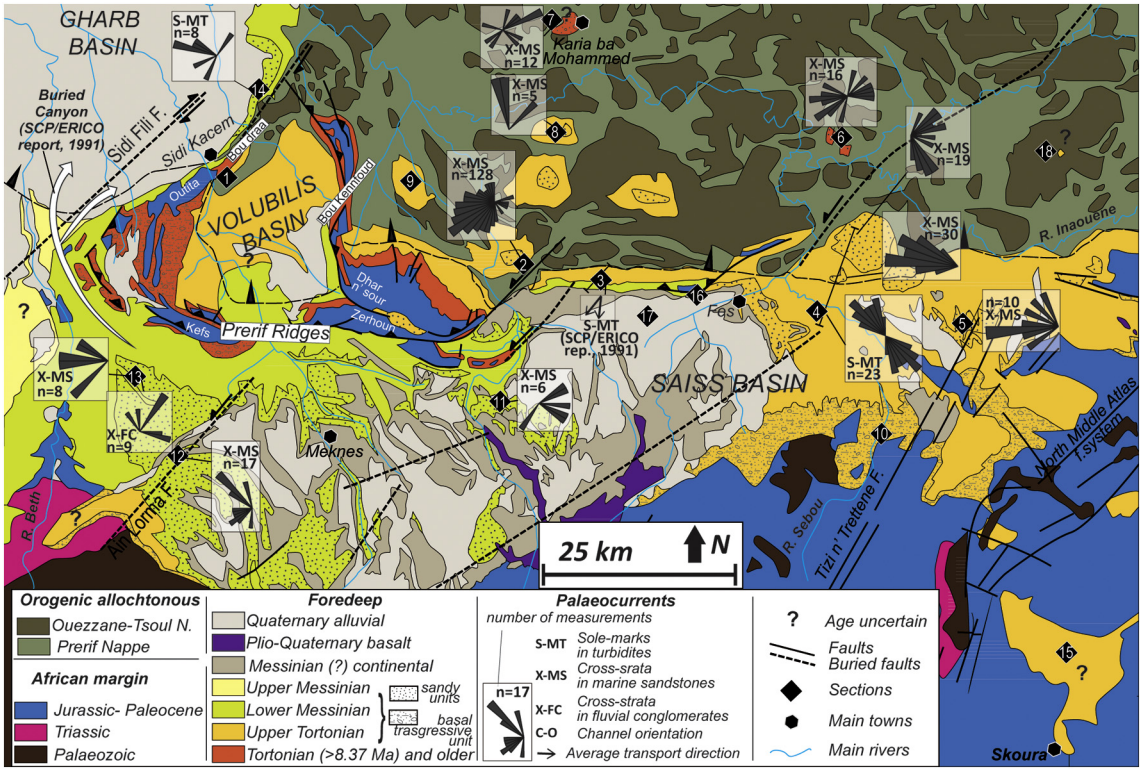


**Fig. 3.** Detailed geological map of the Saiss Basin and the frontal part of the Orogenic wedge with location of major fault systems and studied sections. The subdivision of the Neogene foredeep sediments is based on the results of the present study combined with references cited in text. Colour legend with the pre-Upper Miocene units is shown in Fig. 2. Buried canyon refers to the Upper Miocene and partly Pliocene submarine incision-and-fill mapped with reflection seismic data and interpreted as a contourite moat in (SCP/ERICO report, 1991). Map location in Fig. 1.

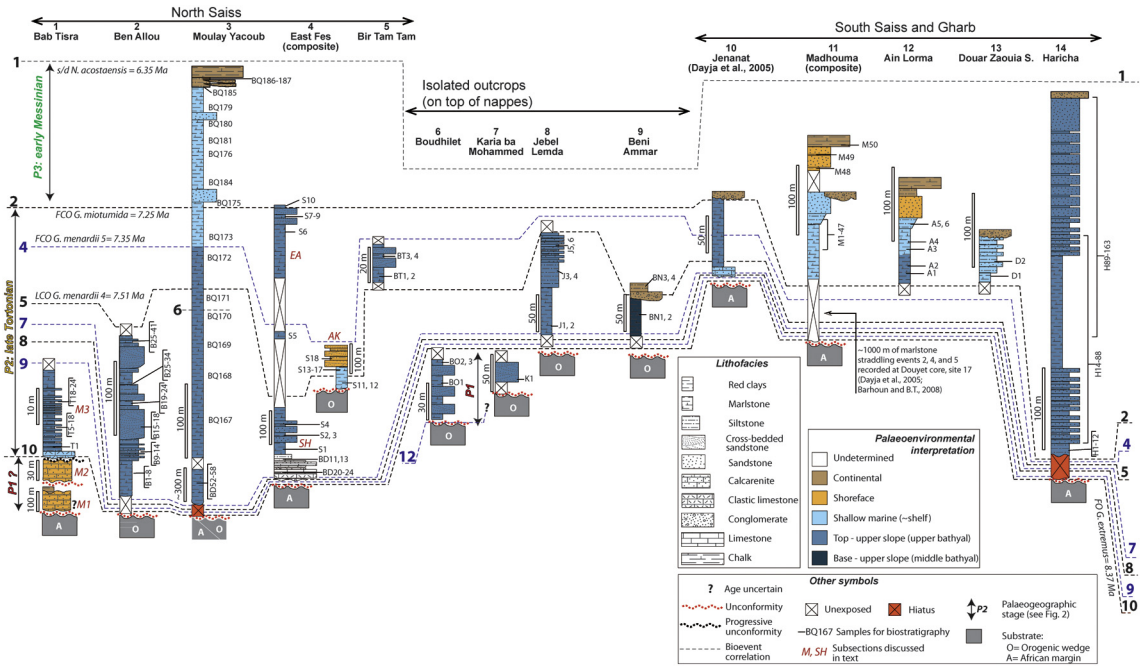


**Fig. 4.** Stratigraphic logs of the studied sections in the Saiss Basin and stratigraphic correlation based on the bioevents shown in Table 1. Lithofacies (symbols) and palaeoenvironmental interpretations (colours) are discussed in the main text and (Capella et al., 2018).

This transgressive event is also recorded at the East Fes section (Figs. 3 and 4; point 4), which is located in the axial foredeep area (set by the Rif nappe thrust front in Fig. 3). At its base, clastic limestones with intervals of sandy marlstones and conglomerates unconformably overlie the African margin. This basal sequence, first analysed by Wernli (Wernli, 1988), is now biostratigraphically dated at a maximum age of 7.92 Ma (Section 1.4 in (Capella et al., 2018)). The basal sequence may therefore represent an initial stage of carbonate platform development that was rapidly drowned by the southward migration of sedimentary environments due to the flexure–controlled subsidence of the foredeep. In more southern areas of the Saiss Basin, different basal facies corresponding to this transgressive event are recorded, namely marginal reefs (Gulf of Skoura; Fig. 3; Point 15) and shallow marine calcarenites (Jenanat; Fig. 4; log 10).

From ca. 8 Ma onwards, the Saiss Basin sedimentation is geographically characterised by widespread deposition of “blue marls” (Figs. 3, 4). The North Saiss Basin, with the Ben Allou, Moulay Yacoub and East Fes sections (Fig. 4; logs 2–4), and the isolated outcrops resting on the orogenic wedge, namely Jebel Lemda and Beni Ammar (Fig. 4; logs 8,9), records upper-slope deposition (water depths of 150–400 m) of marls on top of the frontal part of the orogenic wedge and the African margin. The deepest environment of deposition based on benthic foraminifera is recorded at Beni Ammar (600–800 m) which might represent an enclosed trough on top of the orogenic wedge (Fig. 3). Literature data of the South Saiss Basin (Dayja, 2002) indicates a similar depositional environment of upper bathyal (~150–400 m) facies at the southern margin (Jenanat; Fig. 4; log 10) and centre of the western Saiss Basin (Douyet core; Fig. 3, point 17). A roughly coeval (7.80–7.35 Ma) shoreface (0–50 m) facies is observed at Ain Kansera, subsection of East Fes (AK in log 4; Fig. 4). Here, infralittoral facies (Capella et al., 2017a) would indicate the northern margin of the Saiss Basin, at least during the deposition of this unit (7.80–7.35 Ma). This unit also suggests that emerged areas of the Rifian Corridor existed to the north of Ain Kansera. This is further corroborated by the lack of outcrops on top of the nappe complex to the north. However, it is unclear how much this continental area extended to the north, and how much this palaeo coastline represents only a local shoal or a barely emergent archipelago.

The onset of along-slope bottom currents within the Saiss Basin during the late Tortonian is limited to the northern margin (Fig. 3). West-directed cross-bedding and palaeocurrents derived from the cross-stratified sandstones at Ben Allou and Jebel Lemda (7.80–7.51 Ma), Bir Tam Tam (7.51–7.35 Ma) and East Fes (7.35–7.25 Ma) reflect a seaway–parallel sandy drift at depths of 150–400 m (Capella et al., 2017a).

The Bir Tam Tam section records sandstone transport at upper slope–outer shelf depths. Cross–stratification in sandstone is unidirectional; bioturbation, bioclasts and marine marlstones suggest that the cross–sets are formed by subaqueous dunes. These dunes may reflect either a west–directed bottom current (Anastas et al., 1997; Capella et al., 2017a; Longhitano, 2013) or episodes of sand–laden hyperpycnal flows bypassing river–mouths to the east (Mutti et al., 2003; Tinterri, 2011). The absence of normal turbidites or debrites, typical products of gravity flows, would suggest that these sandstones were probably deposited by bottom-currents.

At El Adergha, subsection of East Fes (EA in log 4; Fig. 4), several hundred m of mud–dominated deposits are interrupted by 20 m thick sandstone units that reflect the onset of contourite deposition in a bottom current-dominated environment (Capella et al., 2017a).

At Ben Allou, bottom–currents were mostly unidirectional and west–directed, as indicated by the nature and orientation of the foresets in cross–stratification (Capella et al., 2017a). The relics of the sandy drifts reveal that, at this location, the currents flowed westward between 7.80 and 7.51 Ma (Fig. 3). A west–directed sandy drift at Ben Allou also suggests that the Saiss Basin communicated with the Gharb Basin north of the Prerif Ridge Dhar n'sour and possibly across Bou Kennfoud (Fig. 3), possibly along the E–W line formed by Beni Ammar (Fig. 3; point 9) and Bab Tisra (Fig. 3; point 1). This is in line with seismic evidence (Capella et al., 2017b; Sani et al., 2007) suggesting that most of the uplift of the Prerif Ridges (Fig. 3) post–dated the late Tortonian. Where the sandstone drift continued to the west of Ben Allou during the late Tortonian remains unclear as the Beni Ammar section only revealed poorly exposed marlstones that could barely provide the information of age and palaeo–depth (Capella et al., 2018).

The Jebel Lemda section represents a crucial control–point for the palaeogeographic reconstruction (Figs. 3, 4; point 8). The alternation of muddy sandstone, muddy siltstones and marlstones may indicate the

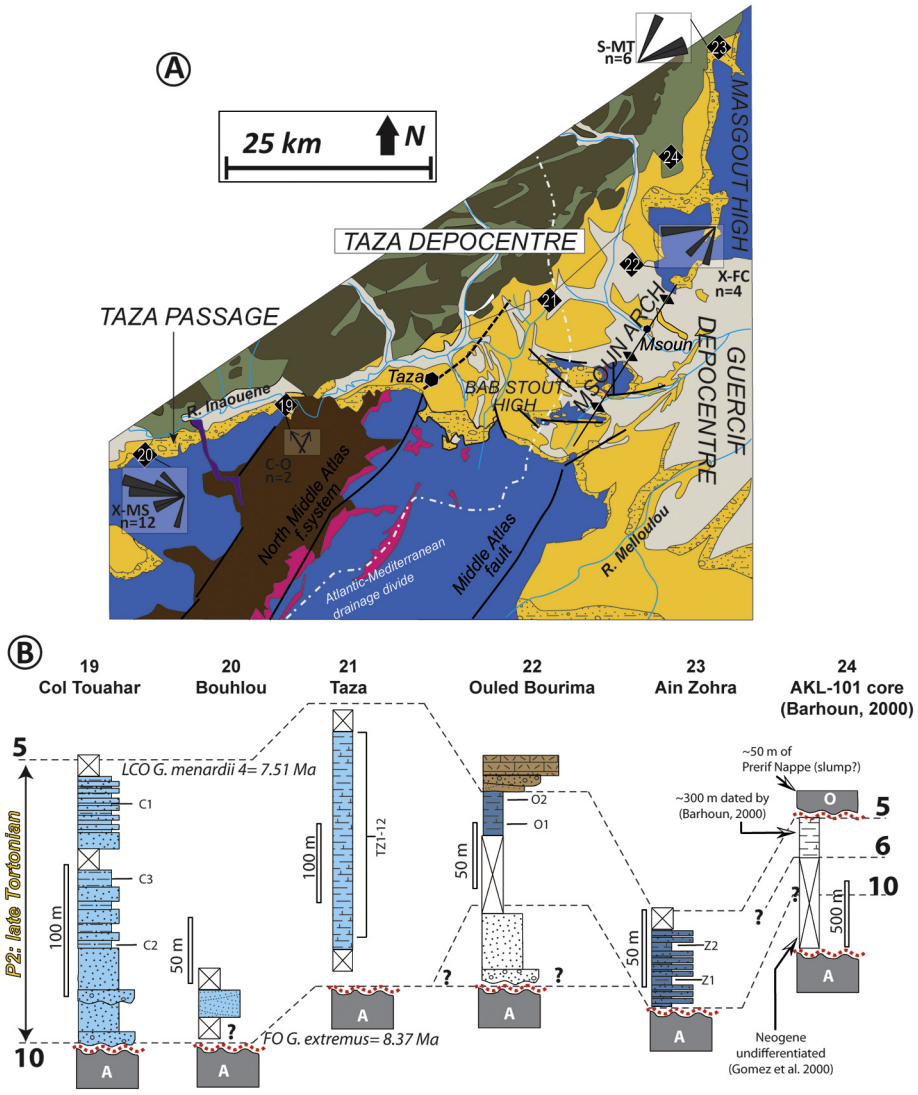


**Fig. 5.** (A) Detailed geological map of the Taza area, with main fault systems and location of the studied sections. The subdivision of the Neogene foredeep sediments is based on the results of the present study combined with references cited in text. Same legend as Fig. 3; map location in Fig. 1. (B) Stratigraphic logs of the studied sections in inset (A) and stratigraphic correlation based on the bioevents shown in Table 1. Same legend as Fig. 4. Lithofacies (symbols) and palaeoenvironmental interpretations (colours) are discussed in the main text and (Capella et al., 2018).

classic, bi-gradational sequence of contouritic deposits (Stow and Faugères, 2008; Stow et al., 1998); Fig. 4N of (Capella et al., 2018)). Given the location of the section between the Saiss and the Had Kourt basins (Fig. 3), this lithofacies suggests that bottom–currents flowed between these two domains. Therefore, this outcrop did not represent the northern margin of the South Rifian Corridor, and marine environments were likely to exist to the north and northwest of this area (Fig. 3).

Lithological changes suggest that from the Tortonian-Messinian boundary onwards, the Saiss Basin underwent substantial re- configuration. The Messinian in the North Saiss Basin is only recorded at one location, Moulay Yacoub (Fig. 4; log 3), in which turbidites with provenance from the north (Fig. 3) are intercalated with the Blue Marl Formation. The Moulay Yacoub section straddles the Tortonian–Messinian boundary and lies on a key location for the study of the evolution of the South Rifian Corridor. The mud–dominated succession reflects sedimentation in an upper bathyal environment during the late Tortonian, with a slight shallowing–upwards trend from the Tortonian–Messinian boundary onwards. At the Tortonian–Messinian boundary the area records the onset of turbidity currents, possibly reflecting an increased tectonic uplift of the source area to the north. The temporal change of foraminiferal assemblage recorded between samples BQ173 and BQ175 could be related to the turbidite sequence that is present roughly at the same interval ((Wernli, 1988); Fig. 4).

We could infer that around the Tortonian–Messinian boundary turbidity currents generated north of Moulay Yacoub and flowed southward on top of the slope formed by the frontal part of the Prerif Nappe (Fig. 3). This piece of evidence would suggest that Moulay Yacoub was not the northern limit of the South Rifian Corridor during the late Tortonian, and that marine environment continued further north. This inference is consistent with the marine character of other patchy exposures of blue marls found above the orogenic wedge to the north (e.g., Jebel Lemda; Fig. 3; point 8).

At Moulay Yacoub, sedimentation rates up to ~100 cm/year$^{-1}$ can be measured between the two samples representing bioevents 4 and 3 (samples BQ 173 and BQ175, respectively). Even higher rates are can be extracted from the intervals between the same bioevents in the contiguous Douyet core (Fig. 3; point 17), namely ~400 cm year$^{-1}$ (Barhoun and Bachiri Taoufiq, 2008) or ~370 cm year$^{-1}$ (Dayja et al., 2005). These exceptionally high rates may include both downslope fill due to tectonic uplift as well as bottom currents (e.g., (Hüneke and Henrich, 2011; Stow and Faugères, 2008)).

In both the East Fes and Jenanat sections (Fig. 4, logs 4, 10) Tortonian sedimentation stops at a level corresponding to the boundary with the Messinian (characterised by the short coexistence of planktic foraminifera *G. menardii* 5 and *G. miotumida*). The top of these two sections is truncated by an unconformity, suggesting that uplift may have started by the Tortonian-Messinian boundary in both the northern and southern margin of the Saiss Basin.

An event of uplift at the Tortonian-Messinian boundary is also in line with the observation that isolated outcrops above the nappe do not record Messinian sedimentation (Fig. 4). Most of the early Messinian marine deposition is limited to the South Saiss Basin and shows a shallowing upward trend towards shelfal and near-shore facies (Madhouma and Ain Lorma sections; Fig. 4, logs 11 and 12). Furthermore, the Madhouma and Ain Lorma sections record the gradual transition from marine to continental-lacustrine deposition. This transition is one of the main subjects of interest in this palaeogeographic study as it indicates the age of closure of the marine connection through the Saiss Basin. The Saiss lacustrine facies were previously reported to be Pliocene in age (Bekkali and Nachite, 2006; Nachite et al., 2003; Wernli, 1988). This Pliocene age was based on the presence of *G. crassaformis* (Dayja et al., 2005; Wernli, 1988) in the transitional, coastal–marine sandy deposits (*Sables fauves* sensu (Wernli, 1988)). This sandy coastal-marine unit is widespread in the Saiss basin; it is found on top of the Messinian part of the Blue Marl Formation, and below the transition to oncolithic freshwater limestone (Taltasse, 1953). We have not found Pliocene species in this unit of the Saiss sections, neither *G. crassaformis,* nor other typical Pliocene foraminifera. In contrast, our results indicate the marine-continental transition took place during the biozone of *G. miotumida* in the early Messinian. This suggests that the uppermost sandy coastal-marine deposits (*sables fauves* in (Boumir, 1990; Dayja et al., 2005; Wernli, 1988)) and most likely also the continental-lacustrine unit above are early Messinian in age as well.

### 4.2. Taza and Guercif depocentres (Fig. 5)

The Taza depocentre is formally part of the Taza-Guercif Basin (e.g., (Gomez et al., 2000; Krijgsman et al., 1999b)), but records a limited sequence due to its confinement by structural highs (Bernini et al., 2000; Gomez et al., 2000). The depocentre extends westwards to the Taza Passage, a narrow band of Upper Miocene sediments that forms the geographical divide between sediments pertaining to the Saiss and the Taza-Guercif Basins (Figs. 1 and 5A). Interestingly, today's geographical divide that separates the watersheds draining into the Mediterranean Sea and into the Atlantic Ocean is not in the Taza Passage, but located 30 km further east (white dotted line in Fig. 5A), suggesting that later uplift reorganized the drainage network.

In the Taza Passage, the onset of clastic sedimentation is recorded at Col Touahar and Bouhlou (Fig. 5; points 19, 20). Conglomerates and sandstones with broadly north-directed palaeocurrents inferred from channels unconformably overlie the Palaeozoic units of the African margin (Fig. 5). The clastic, coarse lithofacies at Col Touahar represent, stratigraphically, the product of the foredeep transgression on the earlier exhumed Atlas domain. These facies associations developed on relatively proximal setting of the shallow ramp (i.e. outer foreland setting) developed on the passive African margin, with respect to an axial foredeep developing further north (Fig. 5A).

At Col Touahar, the large scale (20–50 m in width) channels or conduits (see Fig. 6A, D in (Capella et al., 2018)) are NE and NW orientated, suggesting that flood–dominated deltas were feeding the foredeep from the south, forming a roughly E–W orientated coastline. Bed–scale scours at the base of the wave–reworked turbidites also reflect a NW direction of palaeo-flow (see Fig. 6E in (Capella et al., 2018)). Since these palaeo–current directions indicate the provenance of sediments from a source area located to the south of these outcrops, the roughly ENE–WSW orientated band of sandy sediments at Col Touahar (Fig. 5A) likely represents a good approximation of the orientation of the late Tortonian palaeo–coastline.

In the Taza depocentre *s.s.*, the Blue Marl Formation mainly consists of marlstone with rare sandy intercalations (Fig. 5; point 21). The microfaunal assemblages contained in these marlstones suggest that marine deposition occurred between 8.37 Ma and 7.51 Ma in an outer shelf environment. These marlstones attest to the marine deposition during the late Tortonian in the Taza area, in a depocentre that was partially confined between emergent parts of the Prerif Nappe to the north and the Middle Atlas to the south (Fig. 5A). However, there are no fossil remnants of coeval coastal environments existing to the north of these marlstones. Gomez et al. (Gomez et al., 2000) compiled thickness isopach maps that show a sequence 200 to 400 m thick, composed of upper Tortonian marlstone, located to the west of the town of Msoun, in the Taza depocentre (Fig. 5A). These maps also show that upper Messinian is absent from the Taza depocentre but reaches up to 1200 m in thickness in the Guercif depocentre. According to these authors (Gomez et al., 2000), marine deposition in the Taza depocentre was contrasted by the growth of the Msoun arch (i.e. anticline; Fig. 5A). This arch is represented by the trend of the Middle Atlas fault continuing north, crossing the Bab Stout area and connecting with the Masgout Massif, as suggested also by Chalouan et al. (Chalouan et al., 2014).

The onset of foredeep deposition is also recorded on the Masgout Massif (Fig. 5) in the northeast, which is a northern prolongation of the Middle Atlas. At the contact with the Jurassic, the overlying transgressive facies here consists of calcarenites and sandstones (Ouled Bourima section; Fig. 5, log 22). This part of the basin reaches up to upper bathyal depths (300–500 m water–depth) during the late Tortonian (8.37–7.51 Ma), probably confined by steep slopes, controlled by the Masgout massif (Fig. 5A). The unconformity between the blue marlstones and the continental units at Ouled Bourima (Fig. 6K in (Capella et al., 2018)) suggests that the shallowing of the depocentre occurred rather abruptly, leading to the erosion of part of the blue marlstones by exposure to continental deposition and fluvial events. The fluvial sandstone reflecting fluvial floods directed W and SW–ward would suggest that Masgout was a structural high and the source area of the clastics (Fig. 5A; point 22).

Further north, the Ain Zohra section (8.37–7.51 Ma; point 23) contains turbidite deposits, recording turbidity currents in outer shelf to upper slope environments, based on benthic foraminifera. Ain Zohra turbidites show an immature development of facies ((Mutti et al., 2003); Fig. 6N in (Capella et al., 2018)). This facies association is often observed in foreland basins and represents the transition between the coastal flood–dominated deltas and the deeper, axial foredeep systems (Mutti et al., 2003). Based on sedimentological and micropalaeontological evidence, it is possible that this system developed in distal areas of the shelf or in upper parts of the slope, but relatively proximal areas of the foredeep, near to feeding fan–delta systems or steep confining margins. These feeding areas could have been located either on the Prerif Nappe or the Masgout Massif, or a combination of both. Palaeocurrent patterns from the Ain Zohra section indicate a NE-directed flow, which is roughly parallel to the local orientation of the Rif nappe front, thus suggesting that deeper areas of the foredeep existed north of this location (Figs. 1 and 5A).

The AKL-101 core (Fig. 5; point 24) contains a ~1000 m thick sequence of Neogene sediments unconformably overlying the African margin. Presented as undistinguished Neogene in a subsurface cross-section in Gomez et al. (Gomez et al., 2000), its upper ~300 m have been refined with modern biostratigraphy by Barhoun (Barhoun, 2000) and are now constrained between 7.58 and 7.51 Ma (events 6 and 5, respectively; Table 1). The upper part is overlain by a 50 m thick slump comprising allochtonous material from the Prerif Nappe of the Orogenic Wedge (Fig. 5B; log 24). The AKL–101 core therefore indicates that either gravitational sliding or late movement of the thrust–system has occurred at ca. 7.51 Ma. Due to the age which largely postdated the last movements of the thrust–systems at other locations (ca. 8 Ma), the option of gravitational sliding or slumping is preferred.

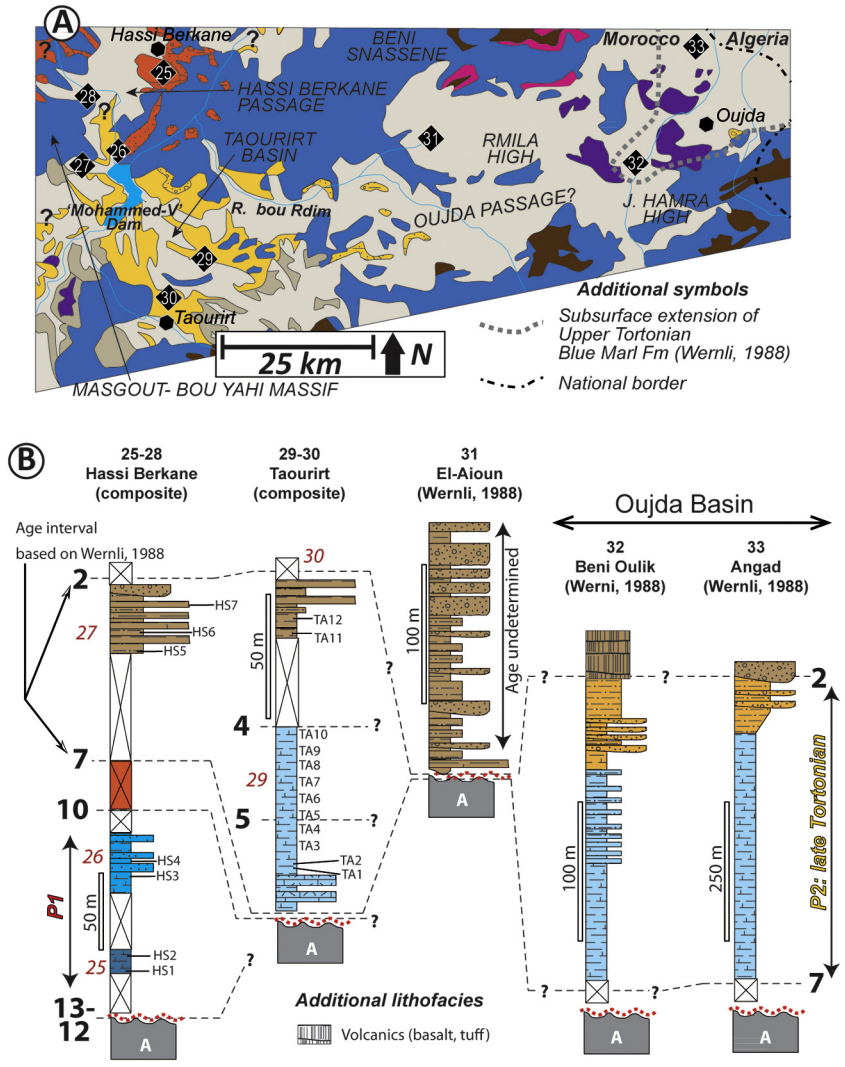


**Fig. 6.** (A) Detailed geological map of the Taourirt–Oujda area with location of the studied sections. The subdivision of the Neogene units is based on the results of the present study combined with references cited in text. Same legend as Fig. 3; map location in Fig. 1. (B) Stratigraphic logs of the studied sections in inset (A) and stratigraphic correlation based on the bioevents shown in Table 1. Same legend as Fig. 4. Lithofacies (symbols) and palaeoenvironmental interpretations (colours) are discussed in the main text and (Capella et al., 2018).

The basal trangressive facies in the Taza Passage reflect the onset of foredeep deposition due to the flexural loading caused by thrust-system reaching the area of the Taza Passage (Fig. 5), whereas the~50 m thick allochtonous material capping the AKL-101 core may reflect a later tectonic pulse during foreland basin infilling. The transition from marine to continental deposits is not continuous in Taza area, and, where present, it shows an erosional unconformity separating marine marls of upper slope water depth (300–500 m) and fluvial sandstone and conglomerate (i.e. Ouled Bourima; Fig. 5, point/log 22).

How the Taza Passage evolved during the early Messinian is unclear, as for the nearest Messinian sediments we have to move laterally ~50 km (East Fes sections and Jenanat in the Saiss, Fig. 3; Guercif depocentre in the Taza–Guercif Basin, Fig. 5A). Another factor of uncertainty is the absence of deep–water facies above the Taza Passage and to the north of it (Fig. 5A), which hints to either erosion or non–-deposition. Furthermore, it is unclear how much of the Upper Miocene sequence overlies the Prerif Nappe or underlies it in a lower structural position.

Unlike the Taza region, the neighbouring Guercif Basin records Messinian deposition (Gomez et al., 2000; Krijgsman et al., 1999b). In Guercif, the basal transgressive unit consists of shallow marine sandstones and mudstones, which are found transgressively overlying the Jurassic basement of the Middle Atlas (Figs. 1 and 5). The sandstones gradually pass into a thick succession of the classical `Blue Marls' showing a cyclic alternation of marls and sandy turbidites with current marks indicative of transport to the north (Bernini et al., 1994; Krijgsman and Langereis, 2000). The upper part of the blue marls is early Messinian in age and contains thick yellow sandy intervals which pass via a number of Ostrea-bearing beds into near-shore and continental sediments (Krijgsman et al., 1999b). The marine deposits along the Zobzit River are biostratigraphically dated to comprise the interval between 8.0 and 6.8 Ma, the continental sediments are considered to be late Messinian and Pliocene in age (Krijgsman et al., 1999b). Neodymium isotope reconstructions of Zobzit samples indicate Mediterranean signals for the Tortonian part of the section, changing towards more Atlantic values in the early Messinian (Ivanovic et al., 2013). This change in neodymium may be related to restriction or closure of the marine connection to the Mediterranean, east of the Taza-Guercif area.

### 4.3. Taourirt–Oujda (Fig. 6)

The depocentres of Taourirt, Hassi-Berkane and Oujda contain Upper Miocene clastic deposits unconformably overlying Jurassic units of the African margin (Wernli, 1988). This area was targeted to better constrain the age of the connections between the Taza-Guercif Basin and the Mediterranean (Fig. 1).

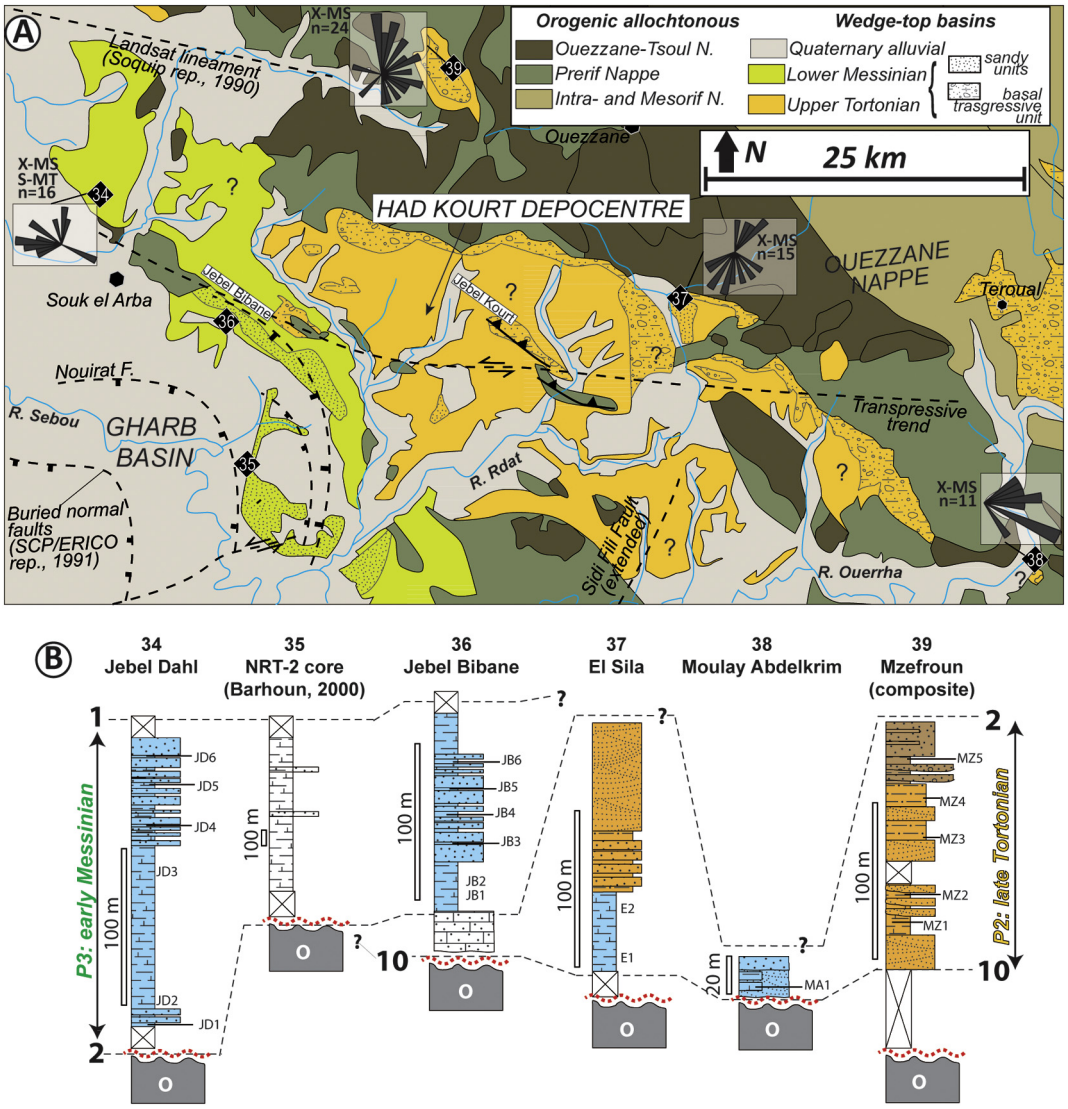


**Fig. 7.** (A) Detailed geological map of the Northern Gharb area, with main fault systems and location of the studied sections. Landsat lineament after Soquip report, 1990. Transpressive trend after (Roest, 2016). Map location in Fig. 1; the symbols not in legend are the same as in Fig. 3. (B) Stratigraphic logs of the studied sections in inset (A) and stratigraphic correlation based on the bioevents shown in Table 1. Same legend as in Fig. 4. Lithofacies (symbols) and palaeoenvironmental interpretations (colours) are discussed in the main text and (Capella et al., 2018).

In outcrops south of Hassi Berkane, the marly units, previously mapped as upper Tortonian (Suter, 1980), are middle Tortonian (10.57–8.37 Ma) in age (point 25, 26 in Fig. 6A, B). They are composed of marlstone with local intercalations of sandstones deposited at upper bathyal depths. The middle Tortonian age of these deposits shows that the marine transgression in the Taourirt–Oujda area is older than in Saiss and Taza-Guercif. At Hassi Berkane, we could not find exposures of sediments belonging to the late Tortonian biozone (8.37–7.25 Ma), although we cannot exclude that they are unexposed or deeply eroded. Wernli (Wernli, 1988) analysed several sets of samples collected in the Hassi Berkane area and reported the presence of upper Tortonian assemblages. What stands out is the presence *G. suterae* and the absence of *G. conomiozea* (Wernli, 1988). These assemblages described in Wernli (Wernli, 1988) could correspond to the biozone between 7.80 and 7.25 Ma (see also Section 3 of (Capella et al., 2018)). It is therefore possible that this narrow and shallow passage connected the Taza–-Guercif Basin to the Mediterranean during the late Tortonian.

The Taourirt depocentre (Fig. 6, points 29–30) shows upper Tortonian (7.80–7.35 Ma) marlstones with rare intercalations of sandstone and indurated layers, revealing mid-outer shelfal depths (100–200 m). The top of the marine sequence grades into lagoonal deposition represented by white chalk, coal-rich layers, and marls poor in microfaunal content. The transition from marine to continental (or lagoonal) environments would suggest a late Tortonian closure for this area. This is consistent with the shoaling trend observed in the Taza–Guercif basin, which highlighted a phase of enhanced uplift starting at the end of the Tortonian (Krijgsman et al., 1999b). The Taourirt depocentre may have been an embayment of the Taza-Guercif Basin that gradually shallowed and became restricted before the Messinian. The closure of the connection between the Taourirt depocentre and the Mediterranean is inferred to have occurred close to the Tortonian-Messinian boundary, in line with the coeval phase of uplift affecting the Taza and Guercif depocentres (Gomez et al., 2000; Krijgsman et al., 1999b).

In the Hassi-Berkane area, the upper Tortonian marlstones with tuff-intercalations as pointed out by Wernli (Wernli, 1988) are difficult to find because of poor exposures. Wernli (Wernli, 1988) reported the presence of *G. suterae* and the absence of *G. conomiozea* in these deposits; an assemblage which could correlate to the late Tortonian age interval between 7.80 and 7.25 Ma.

The Beni Oulik and Angad cores in the Oujda area (Fig. 6; points 32, 33) contain marlstones that increase in siliciclastic input towards the top. Biostratigraphic analyses carried out by Wernli (Wernli, 1988) and

correlated to modern calibrated ages (see discussion at points 3.4 and 3.5 of (Capella et al., 2018)) indicate that this sequence also has a late Tortonian age of 7.80–7.25 Ma. It suggests that a shallow embayment existed in this region, marked by shallow depths at the Beni Oulik core. The Angad core and the Oujda Basin show that Late Miocene open marine conditions existed to the west of the Rmila High (Fig. 6A). Due to the absence of marine sediments in the Rmila High, Wernli (Wernli, 1988) proposed that marine connections were more likely towards the Mediterranean to the east via the Basse–Tafna (Fig. 1) than towards the Taza–Guercif Basin to the west via the Oujda passage.

The Oujda Passage was previously put forward as a major connection of the Rifian Corridor to the Mediterranean (e.g., see Fig. 6 in (Flecker et al., 2015)). However, surface data between the Taourirt and the Oujda depocentre only show continental facies ((Wernli, 1988); Fig. 6A), as well as subsurface data from the El Aioun core (Fig. 6B). This evidence would suggest that the Late Miocene marine transgression did not reach the area. However, we cannot rule out a condensed marine sequence that has subsequently been eroded away. Surface and subsurface data (Wernli, 1988) indicate that the extension of Upper Miocene blue marlstones east of the Taourirt depocentre is limited to the surroundings of Oujda (dotted grey line in Fig. 6A) and further east in Algeria in the Basse–Tafna (Fig. 1). We conclude that connectivity between Oujda and Taza–Guercif depocentres was absent or very restricted; such a narrow sill would have likely generated bottom current–dominated environments, depositing sequences of coarse material as observed in the South (e.g., (Capella et al., 2017a)) or North (e.g., (Achalhi et al., 2016)) Rifian Corridors. However, we cannot exclude that sedimentary products of these vigorous currents remain unfound, underneath the thick continental units that crop out ubiquitously in the area.

### 4.4. Northern Gharb (Fig. 7)

The Northern Gharb area was targeted to better constrain the western mouth of the North Rifian Corridor (Fig. 1) and to detect potential bottom-current or sediment transport pathways. This area is broadly subdivided in an upper Tortonian northeastern part and a Messinian southwestern part. All units unconformably overlie the Prerif nappes of the orogenic wedge, although it remains unclear exactly what part of the Messinian unit overlies the wedge and what part covers a limited and buried sequence of upper Tortonian.

The Had Kourt depocentre represents the northern margin of the Gharb Basin, and its structure at depth has revealed a wedge-top basin reaching up to 2000 m in thickness (Fig. 6 in (Capella et al., 2017b)). The basal units are shallow marine calcarenites that crop out along an E-W transpressive fault trend which forms the Jebel Kourt and Bibane ridges (Fig. 7A). These basal Tortonian units are not directly analysed in this study and we partly rely on the dating of internal reports for their age (SCP/ERICO report, 1991).

The northern and predominantly Tortonian part of the Northern Gharb area, with the El Sila and Mzefroun sections (Fig. 7; points 37, 39), consists of thin sequences of marine, marly deposits capped by coastal sandstone. This transition records a switch from fully marine to near-shore or lagoonal embayment during the upper Tortonian (8.37–7.25 Ma). The embayment may have been flat and sheltered, since the sandstone beds lack HCS and wave cross–bedding as SCS (swaley cross–stratification); however, oyster fragments suggest energetic environment as well as the indications of bidirectional tractive currents observed (points 37 and 39 in Fig. 7; see also Fig. 10D, F in (Capella et al., 2018)). The weathered sandstones commonly found at the top (see Fig. 10C, E, J in (Capella et al., 2018)) could be the product of littoral sand bars and the sand–rich parts of a lagoon–tidal inlet system (Reading and Collinson, 1996).

The coeval Moulay Abdelkrim section (Fig. 7; point 38) consists of massive calcarenites and cross-bedded sandstones (see Fig. 10G in (Capella et al., 2018))indicating east-directed transport (Fig. 7A). Trough–cross bedding at Moulay Abdelkrim is interpreted to reflect 3D subaqueous dunes at relatively shallow depth (~shelf) migrating to the east (Fig. 7B). These deposits may be the product of ebb-tidal currents or Atlantic inflow water flowing eastwards into the Rifian Corridor. Accurate age-control was limited by the high percentage of reworked species, but a Tortonian age is preferred as the marker species of the Messinian (i.e. *G. miotumida*) was not found.

The Messinian units (7.25–6.35 Ma) of the region consist of marlstone, and silty marlstone with variable sandstone intercalations (e.g., see Fig. 10A in (Capella et al., 2018)). At Jebel Dhal and Jebel Bibane (Fig. 7; points 34, 36, respectively), the sandstone and marlstone intercalations are interpreted as the product of a turbidite fan at relatively shallow depth in the foreland basin (outer shelf). The turbidite beds are mostly unchannelised and the sequence thickens upwards, probably indicating progradation of the outer fan. As the palaeocurrent pattern indicates west–directed transport (Fig. 7A; points 34, 36), feeding delta–fronts or sediment–collapse areas were occurring to the north and/or to the east. Minor trends of palaeocurrents towards the north and the east may reflect subordinate palaeo-flows. Main turbidity currents flowing to the southwest are suggested by regional seismic mapping (SCP/ERICO report, 1991; SOQUIP report, 1990). It is possible that the north-directed component of this pattern results from along–slope bottom–currents that veered north at this location (Fig. 12A), and that Jebel Dhal represents a mixed turbidite-contourite system (Mulder et al., 2008). Deeper areas of the slope-apron may be those resulting in the deposition of the NRT-2 core (Fig. 7; point 35), which consists of ~1000 m of mostly marlstone with very few sandstone intercalations deposited between 7.25 and 6.35 Ma (Barhoun, 2000). The NRT–2 core shows that south of the Jebel Dahl – Bibane trend, the Messinian unit is recorded with high thicknesses, probably due a structural low of the Gharb Basin starting at this location. Seismic data (SCP/ERICO report, 1991; SOQUIP report, 1990) suggest that structural lows of the Gharb Basin were controlled by normal faults forming arcs concave to the southwest (Fig. 7A).

Given the shelfal to coastal marine character of the Tortonian deposits found in the northern margin of the Gharb Basin (Fig. 7; points 37–39) and the lack of deposits of Messinian age thereby, this area may have uplifted and emerged during the late Tortonian, as suggested by coeval syndepositional out of sequence thrusting by the Had Kourt ridge (Capella et al., 2017b).

In contrast, substantial extension in the Gharb Basin has been reported in several studies (Flinch, 1993; SCP/ERICO report, 1991; SOQUIP report, 1990; Zouhri et al., 2002) to explain listric normal faults in the Tortonian –Messinian sequences (e.g., Fig. 7A; after (SCP/ERICO report, 1991; SOQUIP report, 1990)). A possibility is that the phase of orogenic exhumation creating uplift and transpressional trends in the Had Kourt–Bibane line (Fig. 7A) was associated with comparable subsidence in the more frontal areas of the Rif nappes to the south, leading to creation of accommodation space that recorded up to 1.5 km of Messinian deposition in the Gharb Basin (see also Section 5). In addition, the process of south-directed extension in the Messinian Gharb (Fig. 7A) might have produced footwall uplift in the Northern Gharb, thus contributing to the shallowing of this area and the closure of the passage to the North Rifian Corridor (Fig. 1).

### 4.5. Intramontane Basins (North Rifian Corridor; Fig. 8)

The Intramontane Basins are a series of interconnected wedge-top basins represented by synformal infills (e.g., (Achalhi et al., 2016; Samaka et al., 1997; Wernli, 1988)) that together formed the northern strand of the Rifian Corridor. A reassessment of the North Rifian Corridor biostratigraphy and basin evolution is presented in Tulbure et al., 2017; here we report the main lithofacies and basin trend.

All basins show a similar coarse basal unit consisting of alternations of marlstone, conglomerate and pebbly sandstone. The basal unit is typically overlain by blue marlstone with irregularly spaced sandy

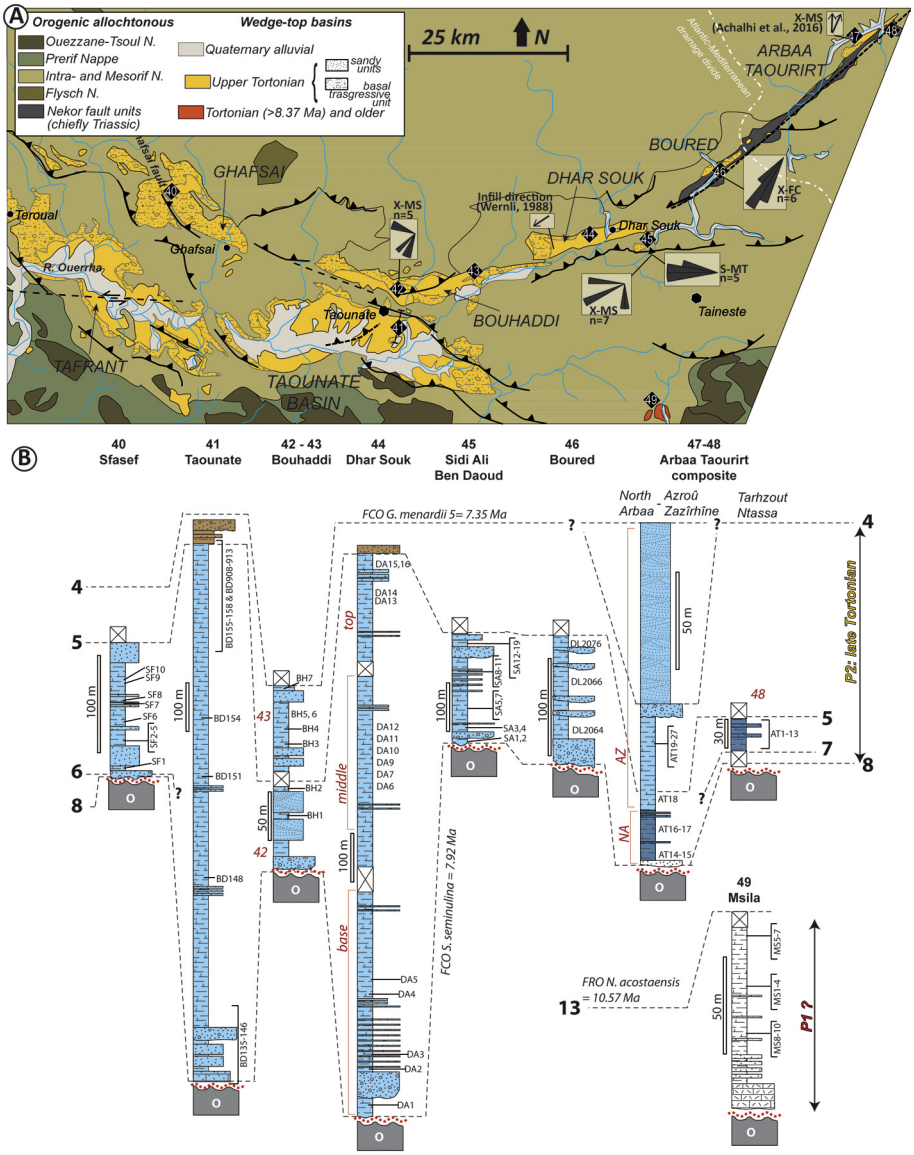


**Fig. 8.** (A) Detailed geological map of the intramontane basins area, with main fault systems and location of the studied sections. Map location in Fig. 1; the symbols not in legend are the same as in Fig. 3. (B) Stratigraphic logs of the studied sections in inset (A) and stratigraphic correlation based on the bioevents shown in Table 1. Same legend as in Fig. 4. Lithofacies (symbols) and palaeoenvironmental interpretations (colours) are discussed in the main text and Tulbure et al., 2017.

intercalations. The marlstone of these basins is characterised by a late Tortonian assemblage (7.92–7.51 Ma), except the Bou Haddi depocentre that records also sediments of the time interval 7.51–7.35 Ma (Fig. 8; point 42–43).

The thickness of the late Tortonian "Blue Marl" successions of the Intramontane Basins varies between 70 and 100 m at Arbaa Taourirt and Boured (Fig. 8; points 46–48) and exceed 1000 m at Taounate and Dhar Souk (Fig. 8; points 41, 44). The top of the marlstone is commonly truncated by erosional unconformities, except at Taounate (Fig. 8, point 41), that records a transition from marine to continental deposition, and Arbaa Taourirt, that records a transition to a shallow marine sandstone and conglomerate unit with northwest-directed palaeo-flow indicators (Fig. 8A; (Achalhi et al., 2016)).

The relative transport directions of palaeoflow indicators constrained in sandstones and conglomerate lobes suggest the area between the Arbaa Taourirt and Boured sections formed a palaeo-sill (Points 46 and 47; Fig. 8A) dividing areas with southwest- and northeast-directed axial drainage. The conglomerate and sandstone lobes in the Taounate, Dhar Souk, Sidi Ali Ben Daoud, and Boured sections (Fig. 8) provide sedimentological evidence of river-dominated submarine fan-deltas and proximal coarse turbidites, which are well-known from foreland settings (e.g., (Mutti et al., 2003)). The intercalated marlstones contain microfaunal assemblages typical of prodelta mud-belts (e.g., *Valvulineria bradyana*; (Amorosi et al., 2013; Goineau et al., 2015)).

The benthic foraminiferal assemblages indicate that depositional environments are generally characterised by depth ranges of 100–250 m, except the Arbaa Taourirt marlstones showing slightly deeper (150–300 m water depth) environments at the base, shallowing upwards to 100–200 m water depth at the top.

Given the age of the marine marlstone between 7.92 and 7.35 Ma and their very high sedimentation rate (minimum rates of 175–244 cm year$^{-1}$) we propose that it is highly unlikely that marls deposition has continued far into the Messinian (Tulbure et al., 2017). The marine-continental transition at the top of the Taounate section (Point 41; Fig. 8) likely records the age of the closure of the North Rifian Corridor, which is estimated to have occurred between 7.35 Ma and the Tortonian-Messinian boundary.

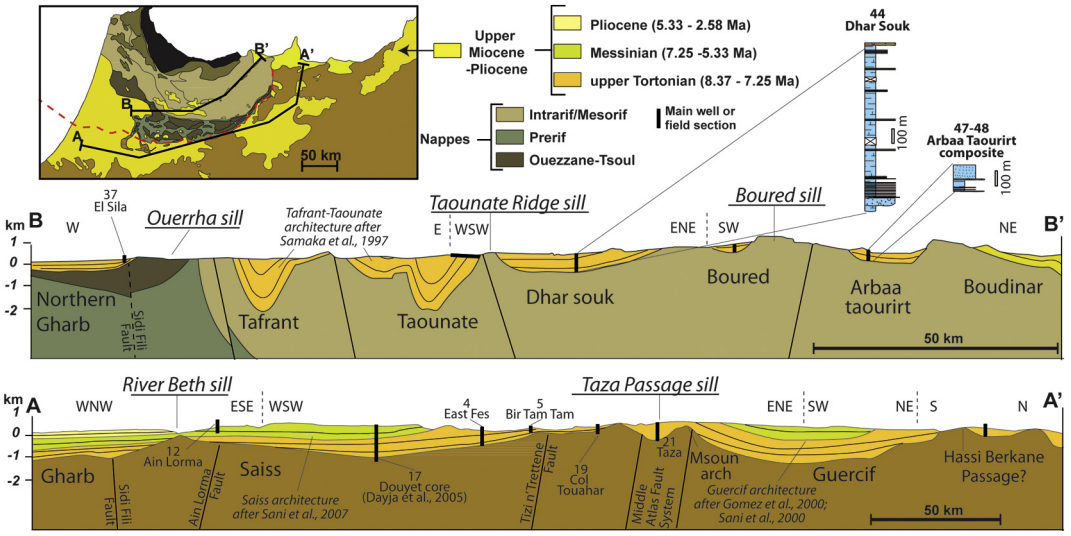


**Fig. 9.** Longitudinal cross-sections illustrating the east to west architecture of the Rifian Corridor in the south (A) and north (B) arms. Palaeo-sills and basins during deposition are constrained by the lateral variation of thicknesses, and the relationship between internal strata and basin margins. The inset map depicts the approximate location of the cross-sections. Additional references for each basin: Vidal, 1979b (Dhar Souk); (SCP/ERICO report, 1991) (Gharb-Oued Beth); (Samaka et al., 1997) (Northern Gharb, Tafrant, Taounate); (Gomez et al., 2000) (Taza-Guercif); (Sani et al., 2000) (Guercif); Azdimousa et al., 2006 (Boudinar); (Sani et al., 2007) (Saiss); (Achalhi et al., 2016) (Arbaa Taourirt, Boudinar).

## 5. Cross-sections derived from subsurface data (Figs. 9–10)

The cross-sections show that most of the sedimentation occurred in depocentres separated by shallow sills (i.e. structural high, horst). This geometry of basin-and-sill is observed both in longitudinal (Fig. 9) and transversal (Fig. 10) cross-sections. Especially in the Intramontane Basins and the frontal part of the Saiss Basin (section D-D′ in Fig. 10), tectonic uplift postdating deposition is evident from the geometry of strata. Basin margins with tilted strata indicate tectonic uplift along high-angle faults, postdating the deposition of the Upper Miocene units. Consequently we infer the following sills limiting depocentres and palaeoflow in the Rifian Corridor:

South Rifian cross-section (A-A′; Fig. 9)

- Oued (=River) Beth sill, consisting of an uplifted area since the late Tortonian (based on the onlap of strata on the sill), controlled by the uplift along inherited structures as the Ain Lorma and Sidi Fili faults (see Fig. 3);
- Taza sill, consisting of two overspill geometries located between the Msoun arch and the Col Touahar;
- Hassi Berkane sill, northern limit of the Taza-Guercif basin, whose age and geometry remains poorly constrained. If we rule out the Oujda Passage, this area must have been a key strait for the connection of the South Rifian corridor to the Mediterranean.

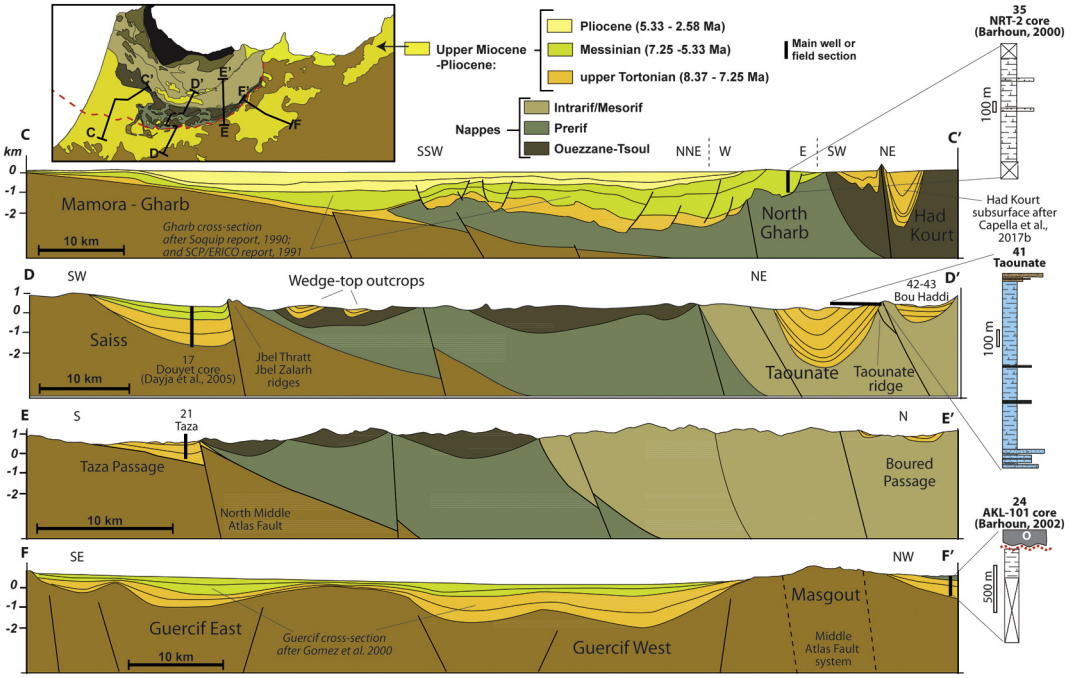


**Fig. 10.** Transverse cross-sections illustrating the north to south architecture of the Rifian Corridor in the Had Kourt–Gharb–Mamora transect (A), Bou Haddi–satellite outcrops–Saiss transect (B), Boured–Taza transect (C). (D) illustrates the architecture of the Taza-Guercif Basin and its relationship with the structural high of Masgout. The insets depict the approximate location of the cross-sections. Additional references for each section: (C-C′) Soquip report, 1990; (SCP/ERICO report, 1991; Zouhri et al., 2002), Zouhri, 2004; (Capella et al., 2017b); (D-D′) (Capella et al., 2017b; Samaka et al., 1997; Sani et al., 2007). (E-E′) (Leblanc, 1978a; Leblanc, 1978b); (F-F′) (Gomez et al., 2000; Sani et al., 2000).

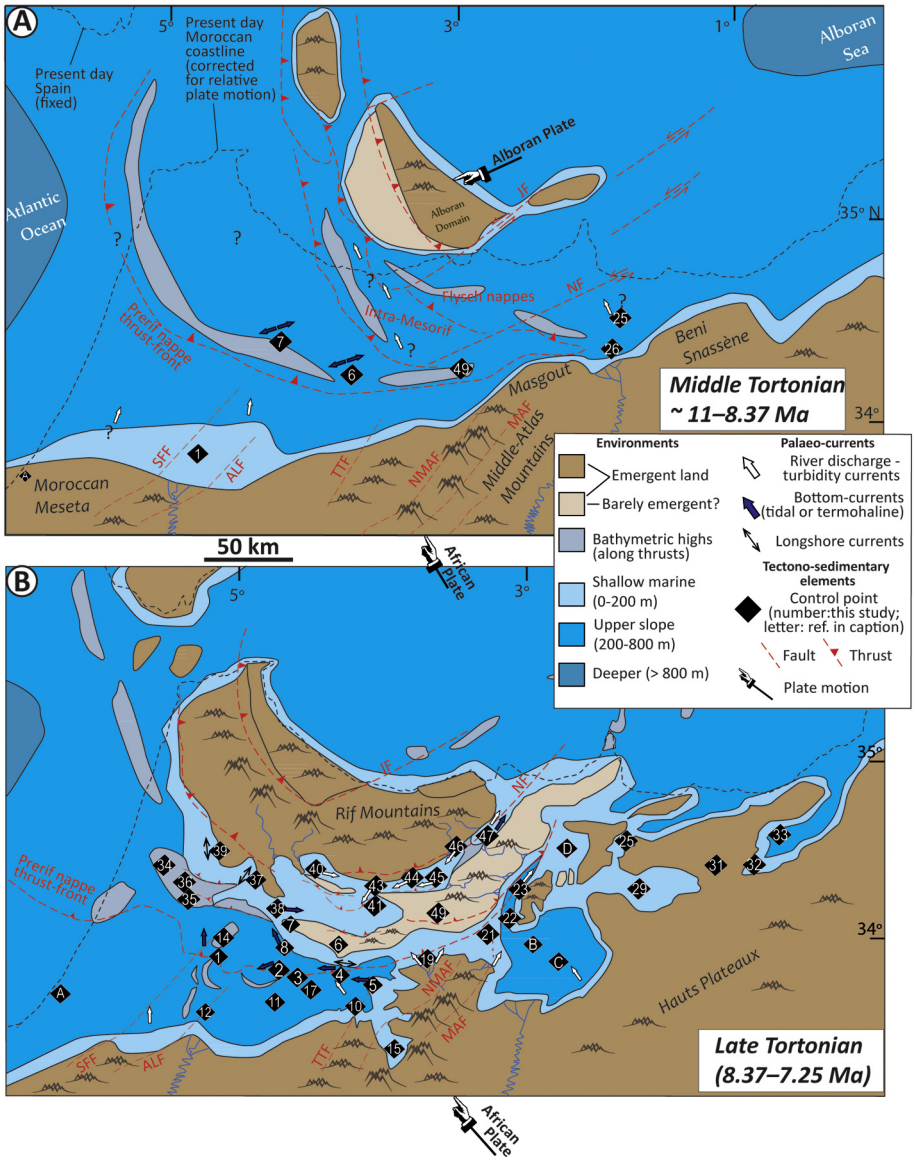


**Fig. 11.** Palaeogeographic evolution and sedimentary environments reconstructions for the Rifian Corridor during the middle Tortonian (A) and late Tortonian (B) with location of the tectonic and orogenic elements controlling basins evolution. Relative sense of plate motions after do Couto et al., 2016; the relative position of Africa respect to fixed Iberia is derived from software GPlates (van Hinsbergen et al., 2014) and is shown schematically with the offset of present-day Moroccan coastline. (A) represents a tentative map of the last phase of thin-skinned tectonics between 11 and 8.37 Ma. The locations of the thrust-systems boundaries are based on the Gibraltar Arc restoration map at ca. 9 Ma presented in (Crespo-Blanc et al., 2016). (B) The Rifian Corridor palaeogeography during the late Tortonian (8.37–7.25 Ma), showing the evolution of the Rif foreland basins after the Miocene westward drift of the Alboran Domain largely ceased (van Hinsbergen et al., 2014; do Couto et al., 2016). Control points in numbers are those in Figs. 3–8 and discussed in the text. Control points based on literature are derived as follows. A: Rabat sections. (Barbieri and Ori, 2000; Hilgen et al., 2000a; Krijgsman et al., 2004). B: MSD1 core, (Barhoun and Bachiri Taoufiq, 2008; Dayja et al., 2005; Dayja, 2002). C: Zobzit–Koudiat Zarga sections, (Krijgsman et al., 1999b). D: South Gareb, Hervouet, 1985. Faults: ALF = Ain Lorma Fault; SFF = Sidi Fili Fault; TTF = Tizi n' Trettene Fault, NMAF = North Middle Atlas Fault; MAF = Middle Atlas Fault; NF = Nekor Fault; JF = Jebha Fault.

North Rifian cross-section (B-B′; Fig. 9)

- Ouerrha sill, located between the intramontane basin of Tafrant and the Had Kourt basin open towards the Atlantic (Figs. 7A and 8A);
- Taounate sill/ridge, controlling connectivity between the Taounate basin and the more internal Bou Haddi and Dhar Souk basins connecting to the Mediterranean via Boured and Arbaa Taourirt (Fig. 7A);
- Boured sill, separating west-directed and east-directed sediment transport (see also Section 4.5);

## 6. Palaeogeographic evolution

### 6.1. Middle Tortonian (Fig. 11A)

The ~500 km wide oceanic corridor between Africa and Iberia underwent a gradual reconfiguration throughout the middle and late Miocene (Do Couto et al., 2016; Jolivet et al., 2006; Van Hinsbergen et al., 2014). Due to the coeval formation of the Betic-Rif thrust-systems (e.g., (Morley, 1993; Platt et al., 2003)) driven by high rates of westward convergence of the Alboran microplate (e.g., (Van Hinsbergen et al., 2014; Vergés and Fernàndez, 2012)), the palaeogeography of the Rifian Corridor was strongly controlled by thin-skinned tectonic processes during the early-middle Tortonian. At that time, the Alboran domain and the African Plate were located at least ~100 km to the east ~72 km to the southwest, respectively, in comparison with the post-8 Ma configurations (Crespo-Blanc et al., 2016; Van Hinsbergen et al., 2014). As a result, ongoing thin-skinned tectonics controlled the migration of thrust barriers and associated depocentres (e.g., (Morley, 1987; Morley, 1988; Morley, 1992; SCP/ERICO report, 1991)).

Consequently, the structural boundaries of the Rif were located further east-northeast as fault propagation in the foreland shifted the location of thrust-top basins. Given such segmented foreland, the basin drainage was likely to follow mostly axial directions, via intersection of the thrust-fronts and associated monoclinal growth folds. The intersection between the accretionary wedge and the passive margin formed a deep trench and several wedge-top or intra-arc basins (Morley, 1988; Morley, 1992), which were likely to be submerged in the accretionary wedge (Fig. 11A).

This configuration led to the deposition of early to middle Tortonian deep-water sandy and clayey sediments that were later incorporated in the thrust-systems (Chalouan et al., 2008; Feinberg, 1986; Morley, 1988; Morley, 1992; Platt et al., 2003). Some exceptions are the para-autochthonous satellite basins of Karia ba Mohammed, Boudhilet

(Fig. 3; points 6 and 7) and Msila (Fig. 8, point 49) which may have recorded deposition on the moving wedge. The southern, marginal equivalents of these wedge-top basins were located in a foreland position on the African margin: examples from this study are the older Miocene units of Bab Tisra (Fig. 3; point 1), and the middle Tortonian at the Hassi Berkane composite section (Fig. 6; points 25 and 26).

### 6.2. Late Tortonian (Fig. 11B)

During the late Tortonian, between 8.37 and 7.92 Ma, the Prerif nappe–thrusts was emplaced in the present day areas of the Saiss and Gharb basins causing flexure of the marginal foreland. The thrust-system was capped by sediments, documenting that thin-skinned tectonic processes had ceased by that time (e.g., (Capella et al., 2017b; Platt et al., 2003)). The flexural loading of the passive African lithosphere generated open marine conditions in large areas of the Mamora, Saiss, and Taza-Guercif basins. This deepening-upward succession is recorded at Bab Tisra (Figs. 3, 4; point 1) and coincides with the late Tortonian transgression observed in the marginal areas of the South Rifian Corridor: the Rabat, Jenanat, Zobzit sections of the Mamora, Saiss, Taza-Guercif basins, respectively (Dayja et al., 2005; Hilgen et al., 2000a; Krijgsman et al., 1999b).

In the intramontane basins, coarse basal sequences are recorded in the basin margins, later uplifted by out of sequence tectonics (e.g., Fig. 8; points 41–46). The North Rifian Corridor developed as a series of interconnected basins limited by thrust fronts and with mostly axial basin drainage (Tulbure et al., 2017), whereas the South Rifian Corridor combined transversal turbidity currents with longitudinal, along-slope bottom-current transport paths (Capella et al., 2017a).

Basin evolution and tectonic control on connectivity are documented by major differences in individual basin stratigraphy and sediment accumulation rates (Figs. 9–10). Palaeoflow in the South Rifian Corridor was controlled by structural highs at key locations, namely the River Beth Sill, the Hassi Berkane and Taza Passages. Similarly, in the North Rifian Corridor most of the sediments accumulated in the main depocentres of Had Kourt, Tafrant, Taounate, Dhar Souk; shallow cross-over zones along the major thrust fronts allowed the basins to be linked along-strike. Steep faulted basin margins lead to the formation of talus cones, alluvial and submarine fans.

The location of steep-faulted structural highs was the most important factor controlling the distribution of upper Tortonian sediments. The Middle Atlas fault in the Taza-Guercif Basin (Fig. 5A), the Tizi n' Trettene and North Middle Atlas faults in the Saiss Basin (Fig. 3), Mount Bou Draa (Fig. 3; see (Sani et al., 2007) for structure at depth),

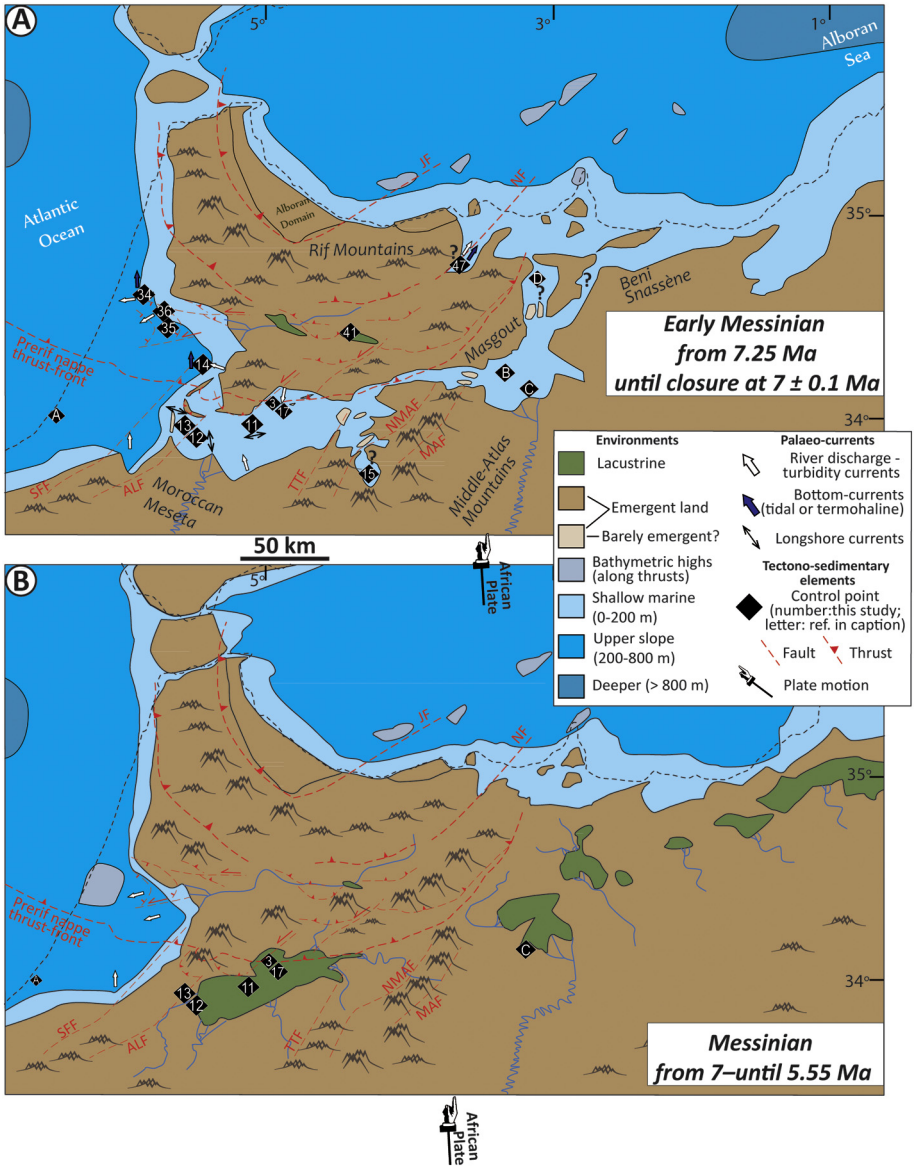


**Fig. 12.** Palaeogeographic evolution and sedimentary environments reconstructions for the Rifian Corridor during the Messinian with location of the tectonic and orogenic elements controlling basins evolution. For faults name see Fig. 11. (A) illustrates the palaeogeography between 7.25 until 7 ± 0.1 Ma, which is the inferred age of closure of the last, southern arm of the Rifian Corridor (see Section 4 in the text for details). (B) is a tentative reconstruction of the Rif foreland palaeogeography and sedimentary environments after the transition from marine to continental deposition. If sedimentation lacks major hiatus, then lacustrine deposits of the Saiss, Guercif, and Taounate Basins are late Messinian in age. Relative sense of plate motions in the Messinian after (Jolivet et al., 2006). Please note that the area of the Strait of Gibraltar in this figure is not part of our reconstruction, and it is only indicative of a potential palaeogeography slighly different than the modern-like, single channel.

and the Sidi Fili fault (Fig. 3) between the Gharb and Saiss basins particularly contributed to the formation of structural highs that may have exerted control on bottom-current flow.

The accretionary slope of the orogenic wedge probably formed a barely emergent archipelago along thrust-fronts, and hosted several intra-slope depocentres that were controlled by active or fossilised thrust surfaces (Fig. 11B). The submerged part is documented by satellite outcrops that record northeast-directed along-slope currents (e.g., Ben Allou, point 2; Jebel Lemda, point 8). The emerged part is indirectly evidenced by near-shore deposits at East Fes (point 4), the direction of turbidity currents inferred from palaeoflow indicators at Ain Zhora in the south (point 23) and Sidi Ali Ben Daoud in the north (point 45).

### 6.3. Early Messinian (Fig. 12A)

During the Messinian, deformation of the Rif foreland recorded a change in tectonic regime consisting in a relative strengthening of the convergence between Africa and Iberia (e.g., (Capella et al., 2017b; Frizon de Lamotte et al., 1991; Jolivet et al., 2006; Morel, 1989)). This tectonic phase, different in nature from the thin-skinned tectonics that created the arc, reactivated the steep faults of the African lithosphere (Capella et al., 2017b; Gomez et al., 2000; Morley, 1987; Sani et al., 2000; Sani et al., 2007) causing localised uplift during the late Tortonian-early Messinian, which further restricted the Rifian Corridor to depocentres limited by shallow sills.

Seismic evidence of steep faults restricting basin sedimentation in the Taounate area (Tulbure et al., 2017) indicates that the North Rifian Corridor shallowed and closed as a result of this phase in the latest Tortonian. We cannot completely rule out that sedimentation continued for a brief time in the Messinian, and subsequently got eroded away, but the high sedimentation rates in the North Rifian Corridor basins make this option arguably very unlikely (see also discussion in Tulbure et al., 2017). Messinian deposition is lacking in all its depocentres, and two areas (Dhar Souk and Arbaa Taourirt) show shallowing trends already starting in the late Tortonian. One area of localised uplift may have been the Taounate Ridge/Sill, as suggested by the tectonic tilt of the layers against its southern margin (Figs. 9 and 10, based on seismic and field evidence presented in Tulbure et al., 2017, and references therein). The Taounate Sill must have been an important cross-over between the more internal areas of the North Rifian Corridor and the Gharb Basin to the west.

There is no section with Messinian deposition on the accretionary slope of the orogenic wedge and no palaeocurrents indicate a possible connection across the Prerif nappes. Hence, we infer that in the early Messinian, the central part of the Rifian Corridor (between the North and South strands) was emerged land, forcing the Mediterranean-Atlantic water exchange through the South Rifian Corridor. In the western part of this emerged land, turbidite deposition occurred in Haricha, at shelf-edge depths with predominantly west-directed transport ((Capella et al., 2017a); Fig. 12A).

During the early Messinian, marine deposition only occurred in the deepest troughs of the South Rifian Corridor: the Guercif, Saiss and Gharb depocentres. The Guercif depocentre reveals palaeoenvironments of deposition equivalent to mid-shelf (50–150 m; (Dayja, 2002; Krijgsman et al., 1999b)); the Saiss depocentre still records marine deposition in its southern sections with similar depth ranges ((Dayja, 2002); Fig. 12A). In the Saiss Basin, congruent events suggesting uplift are recorded at Moulay Yacoub, with onset of turbidite deposition, and at East Fes, with onset of contourite deposition due to a strengthening of the bottom currents possibly reflecting restriction at the sill (Capella et al., 2017a).

The basal part of the Ain Lorma section contains the deepest palaeoenvironment of the lower Messinian sequence, with marlstones reflecting outer shelf to upper slope depths. This sequence grades upwards to shelfal and coastal marine sedimentation that, at its top, records the process of closure with palaeosols and lagoonal to lacustrine carbonate-rich deposition.

Given the continuous nature of the transition from shallow marine to continental deposition in most locations of the South Rifian Corridor, we could calculate an estimated time of the closure based on interpolation of sedimentation rates. These rates are calculated using events 3 and 2 (Table 1); the thickness of marine sediments overlying event 2 and overlain by lacustrine units is then divided by the calculated rate for each of the four successions. Each location shows closure ages as follows.

- Moulay Yacoub (Fig. 4; log 3): rate of 56 cm $ky^{-1}$, leading to an age of closure of 6.96 Ma;
- Douyet core (Fig. 12A; Point 17; (Barhoun and Bachiri Taoufiq, 2008; Dayja et al., 2005)): rate of 260 cm $ky^{-1}$, leading to an age of closure of 7.12 Ma;
- MSD1 core (Fig. 12A; Point B): rate of 180 cm $ky^{-1}$, leading to an age of closure of 6.93 Ma.
- Zobzit–Koudiat Zarga section: (Fig. 12A; Point C; (Krijgsman et al., 1999b)): rate of 220 cm $ky^{-1}$, leading to an age of closure of 6.91 Ma.

These calculated ages are consistent and show that the age of closure of the Rifian Corridor can be confidently constrained at 7.1–6.9 Ma, the Mediterranean–Atlantic connection being completely shut and uplifted. This implies that the age of the continental-lacustrine sediments in the Saiss and the Guercif Basins are Messinian in age, starting from approximately 7.1–6.9 Ma. Our early Messinian palaeogeographic reconstruction shown in Fig. 12A is therefore only valid for the time interval between 7.25 and 7.1–6.9 Ma. After the closure at 7.1–6.9 Ma, the palaeogeography changed to that of the late Messinian (Fig. 12B).

### 6.4. Late Messinian (Fig. 12B)

Marine sediments pertaining to this age interval are only preserved on the Atlantic and Mediterranean side of the corridor, suggesting that marine deposition continued in the Gharb and Boudinar-Melilla basins as embayments of the Atlantic and the Mediterranean, respectively (Fig. 1 and 12B; (Cornée et al., 2016; Krijgsman et al., 2004; Van Assen et al., 2006)).

During the late Messinian, the main deformation process driving basin evolution is Africa-Iberia convergence, concentrating uplift in the areas that were previously the structural highs of the Rifian Corridor; e.g., the sills displayed in the cross–sections (Figs. 9 and 10). During the late Messinian continental deposition was limited to scattered lake areas bounded by topographic highs. Continental-lacustrine sections that were previously regarded as Pliocene (e.g., (Bekkali and Nachite, 2006; Boumir, 1990; Nachite et al., 2003; Wernli, 1988)) may be Messinian in age since they conformably follow the early Messinian marine deposits.

The inherited basin and sill geometry of the Rifian Corridor during the late Messinian generated thick deposits of lacustrine oncolithic limestones that cover great part of the Saiss Basin (Taltasse, 1953), and thick lacustrine-continental successions in the Guercif Basin (Krijgsman and Langereis, 2000; Wernli, 1988). Hence, we infer a Messinian phase of positive fresh-water budget that supplied these former corridor basins with carbonate-rich waters from the Mesozoic units of the Middle Atlas (Nachite et al., 2003; Pratt et al., 2016; Wernli, 1988). The palaeoflow direction of the few outcrops of riverine units where palaeocurrents were measured (X-FC in Fig. 3, point 13; Fig. 5, point 22) is consistent with what is observed today in the Saiss and Taza depocentres (modern rivers in Figs. 3 and 5A, respectively). In conclusion, uncertainties concerning the age of these continental deposits are due to the poor biostratigraphic control and further research will be required to verify the age of the lacustrine formations.

## 7. The Messinian gateway problem

Our field results imply that the connection through Morocco did not contribute to the transport of saline water into the Mediterranean during the Messinian Salinity Crisis. As the seaways through Spain are interpreted to close in the early Messinian as well (Martín et al., 2001) or even before the Tortonian–Messinian boundary according to recent biostratigraphic data (Van der Schee et al., 2018), we conclude that neither Morocco nor Spain records the location of the connection that supplied Atlantic water to the Mediterranean during the primary lower gypsum and the halite stages of the MSC.

Where was then the Messinian gateway that supplied salt into the Mediterranean basin until 5.55 Ma? Both the Rifian and the Betic corridors were closed several hundred thousand years prior to the onset of the Primary Lower Gypsum (PLG) in the Mediterranean (5.97 Ma; (Roveri et al., 2014)). Modelling studies (e.g., (Krijgsman and Meijer, 2008)) have shown that anti-estuarine water exchange is crucial during the PLG in order to sustain Mediterranean basin salinities close to gypsum deposition. Simon and Meijer (Simon and Meijer, 2015) indicated that Atlantic-Mediterranean exchange during the PLG was approximately 25–10% of the present-day value at the Strait of Gibraltar. Their correlation of exchange flux to gateway dimensions indicates that the gateway present prior to a potential disconnection from the Atlantic must have been relatively small (of the order of width ~2–5 km and depth ~20–10 m, if length is taken to be short (~25–50 km)). However, longer gateway length may increase this cross-sectional area due to friction (Simon and Meijer, 2015). Given the longer (43–60 km) morphology of the Strait of Gibraltar at depth (−100 m isobaths; (Blanc, 2002)), a possible but largely unexplored option is the region of the modern Mediterranean-Atlantic connection.

The area of the Gibraltar Straits lacks clear evidence for crustal extension as a driving mechanism for its Pliocene opening; consequently erosional processes are preferred (see review in (Loget and Van Den Driessche, 2006)). However, the Messinian Gibraltar Straits area was likely to be influenced by the evolution of the contiguous Western Alboran Basin, which is thought to record the constant load of the Gibraltar slab throughout the Miocene (Do Couto et al., 2016). During the Tortonian, the Western Alboran Basin documented partial inversions and transpressional structures accompanied by localised subsidence (Comas et al., 1999; Do Couto et al., 2016). Models showed (Govers and Wortel, 2005) that slab sinking would lead to dynamic subsidence, which can occur coevally with regional uplift trends and without requiring surface extension. Slab-sinking in the Gibraltar area has therefore been proposed as the main mechanism to provide the required topographic lowering for the modern Gibraltar Straits to form (Govers, 2009). Given the western Alboran was always affected by the slab-sink (Do Couto et al., 2016), which steepened after the cessation of slab-roll back around ca. 8 Ma (Govers, 2009), we propose that shallow connections through the Strait of Gibraltar were always present. In fact, the only evidence for a Pliocene opening comes from seismic profiles that show canyons cutting into Miocene reflectors in the Alboran Basin. An accurate age determination for these reflectors is lacking, implying that it cannot be completely ruled out that these reflector could have been (partly) formed during the MSC.

We conclude that the Strait of Gibraltar being open during the Messinian is a more plausible scenario than several hundred km long and shallow straits through Morocco and/or Spain. Our reconstructions of the Rifian Corridor, showing an ongoing phase of enhanced uplift in the Rif foreland and the lack of post 7 Ma deposits in the gateway successions, are not supportive of an open MSC connection through Morocco.

## 8. Palaeogeographic evolution: Controlling factors and implications

The palaeogeographic evolution of the Rifian Corridor was strongly influenced by tectonics. The position of reconstructed sills (Figs. 9 and 11), which likely formed bathymetric highs at time of deposition, depends in large part on the trend of inherited Mesozoic faults affecting the African margin. These Mesozoic fault systems caused prominent differences in upper Miocene sediment thicknesses across the corridor basins. Inherited Mesozoic structures affecting the African margin, which are typically SSW-NNE orientated such as the Middle Atlas and the Sidi Fili faults (Figs. 3 and 5), are known to exert a fundamental control on marine facies distribution throughout the Mesozoic (Sani et al., 2007; Zizi, 2002). This study emphasises their role during the late Miocene as well. These structures separate Mesozoic sedimentary successions with great differences in thickness and rheology; therefore, it seems likely that basin subsidence during the Miocene behaved with different intensity on opposite sides of the fault zone (Morley, 1987). For example, the upper Miocene sediments of the Taza-Guercif basin develop to the east of the Middle Atlas fault and not to the west of it (Fig. 1); the Gharb basin and the Saiss basin are limited by the Sidi Fili and Ain Lorma faults, which also contributed to progressive uplift of the areas between the two basins and reorganization of river drainage systems (Fig. 3). The most spectacular result of this process is the Prerif Ridges uplift, a high-topography area largely post-dating the orogen build-up (Capella et al., 2017b; Sani et al., 2007).

Late stage deformation in the Rif foreland may therefore differ substantially from that observed in the Betics. Whereas the relicts of the last connections through the Betics (e.g., Ronda, Antequera, Guadalhorce; see (Martín et al., 2014)) display mostly sub-horizontal layers uplifted to a present day altitude of ~500–700 m, the sedimentary relicts of the north Rifian Corridor are folded and deformed in synclines (Fig. 10 and Tulbure et al., 2017). We infer that late stage contraction deformed these strata by means of reactivation of the high-angle faults rooted in the African margin (Capella et al., 2017b). Thus, in the time of closing seaways, differences in deformation patterns throughout the Gibraltar arc likely depended less to pure Africa-Iberia convergence (Jolivet et al., 2006) than to the complexity of the Gibraltar triple-plate boundary itself.

In the Rifian Corridor, the uplift of bathymetric highs strongly influenced the process of seaway restriction and funnelled tidal and termohaline currents through the straits (Fig. 11), producing sandy contourite deposits in the western part of the seaway analogous to those observed today in the Gulf of Cadiz (points 2,4,5, 8; Fig. 11; (Capella et al., 2017a)). Tectonics is a major controlling factor in the seaway contourite deposition, since it causes the restriction required for the bottom-current to form (Capella et al., 2017a; Hernández-Molina et al., 2016).

If the Rifian Corridor funnelled Mediterranean outflow to an extent analogous to that observed today (Hernández-Molina et al., 2014), then it may have created periodic saline input into the Atlantic centred at mid-depths (Rogerson et al., 2012), thus contributing to the global reorganization of oceanic currents and global climate occurring throughout the middle-late Miocene (Herbert et al., 2016; Lariviere et al., 2012; Potter and Szatmari, 2009).

A broadly similar age of closure (i.e. late Tortonian–early Messinian) of both the Betic and the Rifian Corridors suggests that uplift rates increased simultaneously across the two symmetrical forelands of the Gibraltar arc. Strong uplift rates are required to close the seaways and contrast the strong erosional rates of bottom-currents (Garcia-Castellanos and Villaseñor, 2011). Other parts of the world experienced similar enhanced tectonic activity in the late Miocene, for which a temporal increase in mantle activity and heat flow has been proposed (e.g., (Potter and Szatmari, 2009)). The results of this study therefore emphasise the potential link between geodynamics (mantle convective processes and/or plate convergence associated with seaway closure; (Duggen et al., 2003; Jolivet et al., 2006)) and ocean circulation, already proposed by some for the Greenland-Iceland-Scotland Ridge (e.g., Parnell-Turner et al., 2014) or the Gulf of Cadiz (Hernández-Molina et al., 2014; Hernández-Molina et al., 2016). Both sedimentological

analysis and higher resolution stratigraphy are required to improve the subsurface (i.e. boreholes) age-constraints in the Rifian Corridor, to date syn-kinematic wedges visible in seismic data (e.g., (Capella et al., 2017b)), and possibly to link sandy drift variations to coeval tectonic pulses.

## 9. Conclusions

We provide palaeogeographic reconstructions of depositional environments in the late Miocene sedimentary basins of Northern Morocco based on surface–subsurface correlations, to elucidate the temporal and spatial evolution of the Rifian Corridor. We combined the study of foreland sedimentology and stratigraphy, foreland genesis and evolution (tectonics), and age and palaeoenvironment constraints on the sedimentary successions. From a regional point of view, this paper builds on the work of Feinberg (Feinberg, 1986) and Wernli (Wernli, 1988), and sets the biostratigraphic framework for future studies of the upper Miocene in Northern Morocco or other coeval gateway successions. In a wider perspective, this study emphasises the importance of using consilience between sedimentology, tectonic and dating studies to understand foreland basins and their seaways.

Improved biostratigraphic dating of the more continuous sections and the transitional nature of the basin shallowing show that the Rifian Corridor closed at 7.1–6.9 Ma in the southern strand, and between 7.35 and 7.25 Ma in the northern arm, during a phase of enhanced uplift along high angle faults. The restriction of the corridor started already in the late Tortonian and was driven by the localised uplift of structural highs forming key sills across the longitudinal flow. The position of the highs depends on inherited faults of the Middle Atlas Mountains and Mesozoic grabens in the African margin, which caused prominent differences in sediment thicknesses across the corridor basins. These tectonically controlled highs strongly influenced the corridor restriction and funnelled bottom currents through the straits producing bottom-current dominated environments in the western part of the seaway.

The early Messinian closure of the Rifian Corridor helps explaining the mammal exchanges between Africa and Europe before 6.1 Ma (Agustí et al., 2006; Benammi et al., 1996); on the other hand it requires presence of another Atlantic-Mediterranean gateway to provide the enormous amounts of salt deposited during the MSC between 5.6 and 5.55 Ma (Flecker et al., 2015; Simon and Meijer, 2015; Topper et al., 2011). We conclude that early connections through the Strait of Gibraltar are a possible solution to the Messinian gateway problem.

## Acknowledgements

We thank Roland Wernli (Univ. Genève) for kindly answering our questions and for sending his manuscript, ONHYM for providing prompt assistance, field support and unpublished datasets, the Ministry of Geology in Rabat for allowing us to analyse the sample collections, Abdel Mojid Kouissi (Bab Tiouka commune, Sidi Kacem) for his extraordinary help during several fieldwork campaigns. The research leading to these results has received funding from the People Programme (Marie Curie Actions) of the European Union's Seventh Framework Programme FP7/2007–2013/under REA Grant Agreement No. 290201 (MEDGATE). We are very grateful to all the MEDGATE for the contribution to the fieldwork and all the insightful discussions that enriched this four-year work. Journal reviews by Ed. Paul Wilson and Francisco Javier Hernández-Molina were very much appreciated, and their comments helped us to improve the clarity of the manuscript.

## References

Achalhi, M., Münch, P., Cornée, J.J., Azdimousa, A., Melinte-Dobrinescu, M., Quillévéré, F., Drinia, H., Fauquette, S., Jiménez-Moreno, G., Merzeraud, G., Moussa, A.B., 2016. The late Miocene Mediterranean-Atlantic connections through the North Rifian Corridor: new insights from the Boudinar and Arbaa Taourirt basins (northeastern Rif, Morocco). Palaeogeogr. Palaeoclimatol. Palaeoecol. 459, 131–152.

Agustí, J., Garcés, M., Krijgsman, W., 2006. Evidence for African–Iberian exchanges during the Messinian in the Spanish mammalian record. Palaeogeogr. Palaeoclimatol. Palaeoecol. 238 (1–4), 5–14.

Amorosi, A., Rossi, V., Vella, C., 2013. Stepwise post-glacial transgression in the Rhône Delta area as revealed by high-resolution core data. Palaeogeogr. Palaeoclimatol. Palaeoecol. 374, 314–326.

Anastas, A.S., Dalrymple, R.W., James, N.P., Nelson, C.S., 1997. Cross-bedded calcarenites from New Zealand: subaqueous dunes in a cool-water Oligo-Miocene seaway. Sedimentology 44, 869–891.

Azdimousa, A., Poupeau, G., Rezqi, H., Asebriy, L., Bourgois, J., Aït Brahim, L., 2006. Géodynamique des bordures méridionales de la mer d'Alboran; application de la stratigraphie séquentielle dans le bassin néogène de Boudinar (Rif oriental, Maroc). Bulletin de l'Institut Scientifique, Rabat, section Sciences de la Terre 28, 9–18.

Barbieri, R., Ori, G.G., 2000. Neogene palaeoenvironmental evolution in the Atlantic side of the Rifian Corridor (Morocco). Palaeogeogr. Palaeoclimatol. Palaeoecol. 163, 1–31.

Barhoun, N., 2000. Biostratigraphie et paléoenvironnement du Miocène supérieur et du Pliocène inférieur du Maroc septentrional: apport des foraminifères planctoniques. Thèse d'état des Sciences, université Hassan II-Mohammedia, Casablanca, Maroc (272 p.).

Barhoun, N., Bachiri Taoufiq, N., 2008. Événements biostratigraphiques et environnementaux enregistrés dans le corridor sud rifain (Maroc septentrional) au Miocène supérieur avant la crise de salinité messinienne. Geodiversitas 1 (30), 21–40.

Bekkali, R., Nachite, D., 2006. Le bassin lacustre-palustre plio-pleistocène de Saïss: ostracodes et paléohydrochimie. In: Aperçu sur les ostracodes du Néogène récent du Nord-Ouest Marocain. Ostracodes et Paléoenvironnement. Laboratoire de Cartographie et de Gestion Environnementale et Marine, Universit Abdelmalek Essaadi, Tetouan, pp. 63–81.

Benammi, M., Calvo, M., Prevot, M., Jaeger, J.J., 1996. Magnetostratigraphy and paleontology of Ait Kandoula Basin (High Atlas, Morocco) and the African–European late Miocene terrestrial fauna exchanges. Earth Planet. Sci. Lett. 145 (1–4), 15–29.

Benson, R.H., Rakic-El Bied, K., Bonaduce, G., 1991. An important current reversal (influx) in the Rifian corridor (Morocco) at the Tortonian–Messinian Boundary: the end of Tethys Ocean. Paleoceanography 6 (1), 165–192.

Bernini, M., Boccaletti, M., El Mokhtari, J., Gelati, R., Moratti, G., Papani, G., 1994. Geologic-structural map of the Taza-Guercif Neogene basin (north-eastern Morocco). In: Scale 1:50,000. S.El.Ca, Firenze.

Bernini, M., Boccaletti, M., Moratti, G., Papani, G., 2000. Structural development of the Taza-Guercif Basin as a constraint for the Middle Atlas Shear Zone tectonic evolution. Mar. Pet. Geol. 17 (3), 391–408.

Bertotti, G., Mosca, P., Juez, J., Polino, R., Dunai, T., 2006. Oligocene to present kilometres scale subsidence and exhumation of the Ligurian Alps and the Tertiary Piedmont Basin (NW Italy) revealed by apatite (U-Th)/He thermochronology: correlation with regional tectonics. Terra Nova 18, 18–25.

Blanc, P.L., 2002. The opening of the Plio-Quaternary Gibraltar Strait: assessing the size of a cataclysm. Geodin. Acta 15 (5–6), 303–317.

Boumir, K., 1990. Paléoenvironnements de dépôt et transformations postsédimentaires des sables fauves du bassin de Sais (Maroc). In: Thèse doctoral. Université Nancy I, pp. 1–176.

Capella, W., Hernández-Molina, F.J., Flecker, R., Hilgen, F.J., Hssain, M., Kouwenhoven, T.J., van Oorschot, M., Sierro, F.J., Stow, D.A.V., Trabucho-Alexandre, J., Tulbure, M.A., de Weger, W., Yousfi, M.Z., Krijgsman, W., 2017a. Sandy contourite drift in the late Miocene Rifian Corridor (Morocco): reconstruction of depositional environments in a foreland-basin seaway. Sediment. Geol. http://dx.doi.org/10.1016/j.sedgeo.2017.04.004.

Capella, W., Matenco, L., Dmitrieva, E., Roest, W.M.J., Hessels, S., Hssain, M., Chakor-Alami, A., Sierro, F.J., Krijgsman, W., 2017b. Thick-skinned tectonics closing the Rifian Corridor. Tectonophysics. http://dx.doi.org/10.1016/j.tecto.2016.09.028.

Capella, W., Barhoun, N., Flecker, R., Hilgen, F.J., Kouwenhoven, T., Matenco, L.C., Sierro, F.J., Tulbure, M.A., Yousfi, M.Z., Krijgsman, W., 2018. Lithofacies, Sedimentology and Palaeontology of South Rifian Corridor Sections (Morocco). (Data in Brief, submitted).

Chalouan, A., Michard, A., El Kadiri, K., Negro, F., Frizon de Lamotte, D., Soto, J.I., Saddiqi, O., 2008. The Rif Belt. In: Michard, A., Saddiqi, O., Chalouan, A., Frizon de Lamotte, D. (Eds.), Continental Evolution: The Geology of Morocco. Lecture Notes in Earth Sciences, Springer-Verlag, Berlin, pp. 203–302.

Chalouan, A., Gil, A.J., Galindo-Zaldívar, J., Ruano, P., de Lacy, M.C., Ruiz-Armenteros, A.M., Benmakhlouf, M., Riguzzi, F., 2014. Active faulting in the frontal Rif Cordillera (Fes region, Morocco): constraints from GPS data. J. Geodyn. 77, 110–122.

Charrière, A., Saint-Martín, J.P., 1989. Relations entre les formations récifales du Miocène supérieur et la dynamique d'ouverture et de fermeture des communications marines à la bordure méridionale du sillon sud-rifain (Maroc). C. R. Acad Sci II 309, 611–614.

Cirac, P., 1987. Le bassin sud-rifain occidental au Néogène supérieur. Mémoires de l'Institut de Géologie du Bassin d'Aquitaine 21.

Comas, M.C., Platt, J.P., Soto, J.I., Watts, A.B., 1999. The origin and tectonic history of the Alboran basin: insights from leg 161 results. Proc. Ocean Drill. Program Sci. Results 161, 555–580.

Cornée, J.J., Münch, P., Achalhi, M., Merzeraud, G., Azdimousa, A., Quillévéré, F., Melinte Dobrinescu, M., Chaix, C., Ben Moussa, A., Lofi, J., Séranne, M., Moissette, P., 2016. The Messinian erosional surface and the early Pliocene reflooding in the Alboran Sea: new insights from the Boudinar basin, Morocco. Sediment. Geol. 333, 115–129.

Crespo-Blanc, A., Comas, M., Balanyá, J.C., 2016. Clues for a Tortonian reconstruction of the Gibraltar Arc: structural pattern, deformation diachronism and block rotations.

Tectonophysics 683, 308–324.
Dayja, D., 2002. Les foraminifères néogènes, témoins de la chronologie, de la bathymétrie et de l'hydrologie du Corridor Rifain (Maroc septentrional). Doctoral dissertation, Paris 6.
Dayja, D., Janin, M.C., Boutakiout, M., 2005. Biochronologie et corrélation des bassins néogènes du Couloir sud-rifain (Maroc) fondées sur les évènements de foraminifères planctoniques et de nannofossiles calcaires. Rev. Micropaleontol. 48 (3), 141–157.
Do Couto, D., Gorini, C., Jolivet, L., Lebret, N., Augier, R., Gumiaux, C., d'Acremont, E., Ammar, A., Jabour, H., Auxietre, J.L., 2016. Tectonic and stratigraphic evolution of the Western Alboran Sea Basin in the last 25Myrs. Tectonophysics 677, 280–311.
Duggen, S., Hoernie, K., van den Bogaard, P., Rupke, L., Phipps Morgan, J., 2003. Deep roots of the Messinian salinity Crisis. Nature 422, 602–606.
Feinberg, H., 1978. Evolution paleogéographique de l'avant-pays du Rif (Maroc) pendant le Miocène supérieur. Mémoires du Mus. Natn. Hist. Nat., Paris (518), 149–155.
Feinberg, H., 1986. Les séries tertiaires des zones externes du Rif (Maroc); biostratigraphie, paléogéographie et aperçu tectonique. Notes et Mémoires du Service Géologique du Maroc 315, 192.
Flecker, R., Krijgsman, W., Capella, W., de Castro Martíns, C., Dmitrieva, E., Mayser, J.P., Marzocchi, A., Modestou, S., Ochoa, D., Simon, D., Tulbure, M., van den Berg, B., van der Schee, M., de Lange, G., Ellam, R., Govers, R., Gutjahr, M., Hilgen, F., Kouwenhoven, T., Lofi, J., Meijer, P., Sierro, F.J., Bachiri, N., Barhoun, N., Alami, A.C., Chacon, B., Flores, J.A., Gregory, J., Howard, J., Lunt, D., Ochoa, M., Pancost, R., Vincent, S., Yousfi, M.Z., 2015. Evolution of the Late Miocene Mediterranean–Atlantic gateways and their impact on regional and global environmental change. Earth Sci. Rev. 150, 365–392.
Flinch, F.J., 1993. Tectonic evolution of the Gibraltar Arc [Unpubl. Ph.D. Thesis]. Rice University, Houston (381 p.).
Foresi, L.M., Bonomo, S., Caruso, A., Di Enrico, S., Salvatorini, G., Sprovieri, R., 2002. Calcareous plankton high resolution biostratigraphy (foraminifera and nannofossils) of the uppermost Langhian-lower Serravallian Ras il-Pellegrin section (Malta). Riv. Ital. Paleontol. Stratigr. 108, 195–210.
Frizon de Lamotte, D., Andrieux, J., Guezou, J.C., 1991. Cinematique des chevauchements neogenes dans l'Arc betico-rifain; discussion sur les modeles geodynamiques. Bull. Soc. Geol. Fr. 162, 611–626.
Garcia-Castellanos, D., Villaseñor, A., 2011. Messinian Salinity Crisis regulated by competing tectonics and erosion at the Gibraltar arc. Nature 480, 359–363.
Gelati, R., Moratti, G., Papani, G., 2000. The Late Cenozoic sedimentary succession of the Taza-Guercif Basin, South Rifian Corridor, Morocco. Mar. Pet. Geol. 17 (3), 373–390.
Goineau, A., Fontanier, C., Mojtahid, M., Fanget, A.-S., Bassetti, M.-A., Berné, S., Jorissen, F., 2015. Live–dead comparison of benthic foraminiferal faunas from the Rhône prodelta (Gulf of Lions, NW Mediterranean): development of a proxy for palaeoenvironmental reconstructions. Mar. Micropaleontol. 119, 17–33.
Gomez, F., Barazangi, M., Demnati, A., 2000. Structure and evolution of the Neogene Guercif Basin at the junction of the Middle Atlas Mountains and the Rif Thrust Belt, Morocco. AAPG Bull. 84 (9), 1340–1364.
Govers, R., 2009. Choking the Mediterranean to dehydration: the Messinian Salinity Crisis. Geology 37 (2), 167–170.
Govers, R., Wortel, M.J.R., 2005. Lithosphere tearing at STEP faults: response to edges of subduction zones. Earth Planet. Sci. Lett. 236 (1), 505–523.
Herbert, T.D., Lawrence, K.T., Tzanova, A., Peterson, L.C., Caballero-Gill, R., Kelly, C.S., 2016. Late Miocene global cooling and the rise of modern ecosystems. Nat. Geosci. 9, 843–847.
Hervouet, Y., 1985. Evolution tectono-sédimentaire de l'avant-fosse Rifaine du Maroc oriental au Miocène. Bulletin de l'institut Scientifique de Rabat 9, 81–88.
Hernández-Molina, F.J., Llave, E., Preu, B., Ercilla, G., Fontan, A., Bruno, M., Serra, N., Gomiz, J.J., Brackenridge, R.E., Sierro, F.J., Stow, D.A., 2014. Contourite processes associated with the Mediterranean Outflow Water after its exit from the Strait of Gibraltar: global and conceptual implications. Geology 42 (3), 227–230.
Hernández-Molina, F.J., Sierro, F.J., Llave, E., Roque, C., Stow, D.A.V., Williams, T., Lofi, J., Van der Schee, M., Arnáiz, A., Ledesma, S., Rosales, C., 2016. Evolution of the gulf of Cadiz margin and southwest Portugal contourite depositional system: tectonic, sedimentary and paleoceanographic implications from IODP expedition 339. Mar. Geol. 377, 7–39.
Hilgen, F.J., Krijgsman, W., 1999. Cyclostratigraphy and astrochronology of the Tripoli diatomite formation (pre-evaporite Messinian, Sicily, Italy). Terra Nova-Oxford 11 (1), 16–22.
Hilgen, F.J., Krijgsman, W., Langereis, C.G., Lourens, L.J., Santarelli, A., Zachariasse, W.J., 1995. Extending the astronomical (Polarity) time scale into the Miocene. Earth Planet. Sci. Lett. 136, 495–510.
Hilgen, F., Bissoli, L., Iaccarino, S., Krijgsman, W., Meijer, R., Negri, A., Villa, G., 2000a. Integrated stratigraphy and astrochronology of the Messinian GSSP at Oued Akrech (Atlantic Morocco). Earth Planet. Sci. Lett. 182 (3), 237–251.
Hilgen, F.J., Krijgsman, W., Raffi, I., Turco, E., Zachariasse, W.J., 2000b. Integrated stratigraphy and astronomical calibration of the Serravallian/Tortonian boundary section at Monte Gibliscemi (Sicily, Italy). Mar. Micropaleontol. 38 (3), 181–211.
Hüneke, H., Henrich, R., 2011. Pelagic sedimentation in modern and ancient oceans. In: Hüneke, H., Mulder, T. (Eds.), Deep-sea Sediments. Elsevier, Amsterdam, The Netherlands, pp. 215–351.
Hüsing, S.K., Kuiper, K.F., Link, W., Hilgen, F.J., Krijgsman, W., 2009a. The upper Tortonian–lower Messinian at Monte dei Corvi (Northern Apennines, Italy): completing a Mediterranean reference section for the Tortonian stage. Earth Planet. Sci. Lett. 282, 140–157.
Hüsing, S.K., Zachariasse, W.J., Van Hinsbergen, D.J.J., Krijgsman, W., Inceöz, M., Harzhauser, M., Mandic, O., Kroh, A., 2009b. Oligocene-Miocene basin evolution in SE Anatolia, Turkey: constraints on the closure of the eastern Tethys gateway. Geol. Soc. Lond., Spec. Publ. 311, 107–132.
Hüsing, S.K., Oms, O., Agusti, J., Garces, M., Kouwenhoven, T.J., Krijgsman, W., Zachariasse, W.J., 2010. On the late Miocene closure of the Mediterranean-Atlantic gateway through the Guadix basin (southern Spain). Palaeogeogr. Palaeoclimatol. Palaeoecol. 291 (3–4), 167–179.
Ivanovic, R.F., Flecker, R., Gutjahr, M., Valdes, P.J., 2013. First Nd isotope record of Mediterranean–Atlantic water exchange through the Moroccan Rifian Corridor during the Messinian Salinity Crisis. Earth Planet. Sci. Lett. 368, 163–174.
Jolivet, L., Augier, R., Robin, C., Suc, J.P., Rouchy, J.M., 2006. Lithospheric-scale geodynamic context of the Messinian Salinity Crisis. Sediment. Geol. 188, 9–33.
Kouwenhoven, T.J., Hilgen, F.J., Van der Zwaan, G.J., 2003. Late Tortonian–early Messinian stepwise disruption of the Mediterranean–Atlantic connections: constraints from benthic foraminiferal and geochemical data. Palaeogeogr. Palaeoclimatol. Palaeoecol. 198, 303–319.
Kouwenhoven, T.J., Morigi, C., Negri, A., Giunta, S., Krijgsman, W., Rouchy, J.M., 2006. Paleoenvironmental evolution of the eastern Mediterranean during the Messinian: constraints from integrated microfossil data of the Pissouri Basin (Cyprus). Mar. Micropaleontol. 60, 17–44 (Krijgsman and Garcés, 2004).
Krijgsman, W., Garcés, M., 2004. Palaeomagnetic constraints on the geodynamic evolution of the Gibraltar Arc. Terra Nova 16 (5), 281–287.
Krijgsman, W., Langereis, C.G., 2000. Magnetostratigraphy of the Zobzit and Koudiat Zarga sections (Taza-Guercif basin, Morocco): implications for the evolution of the Rifian Corridor. Mar. Pet. Geol. 17, 359–371.
Krijgsman, W., Meijer, P.T., 2008. Depositional environments of the Mediterranean "Lower Evaporites" of the Messinian Salinity Crisis: constraints from quantitative analyses. Mar. Geol. 253, 73–81.
Krijgsman, W., Hilgen, F.J., Langereis, C.G., Santarelli, A., Zachariasse, W.J., 1995. Late Miocene magnetostratigraphy, biostratigraphy and cyclostratigraphy in the Mediterranean. Earth Planet. Sci. Lett. 136 (3–4), 475–494.
Krijgsman, W., Hilgen, F.J., Negri, A., Wijbrans, J.R., Zachariasse, W.J., 1997. The Monte del Casino section (Northern Apennines, Italy): a potential Tortonian/Messinian boundary stratotype? Palaeogeogr. Palaeoclimatol. Palaeoecol. 133 (1–2), 27–47.
Krijgsman, W., Hilgen, F.J., Raffi, I., Sierro, F.J., Wilson, D.S., 1999a. Chronology, causes and progression of the Messinian Salinity Crisis. Nature 400 (6745), 652–655.
Krijgsman, W., Langereis, C.G., Zachariasse, W.J., Boccaletti, M., Moratti, G., Gelati, R., Iaccarino, S., Papani, G., Villa, G., 1999b. Late Neogene evolution of the Taza-Guercif Basin (Rifian Corridor, Morocco) and implications for the Messinian Salinity Crisis. Mar. Geol. 153, 147–160.
Krijgsman, W., Gaboardi, S., Hilgen, F.J., Iaccarino, S., Kaenel, E.D., Laan, E.V.D., 2004. Revised astrochronology for the Ain el Beida section (Atlantic Morocco): no glacio-eustatic control for the onset of the Messinian Salinity Crisis. Stratigraphy 1, 87–101.
Lariviere, J.P., Ravelo, A.C., Crimmins, A., Dekens, P.S., Ford, H.L., Lyle, M., Wara, M.W., 2012. Late Miocene decoupling of oceanic warmth and atmospheric carbon dioxide forcing. Nature 486, 97–100. http://dx.doi.org/10.1038/nature11200.
Leblanc, D., 1978a. Carte Géologique du Maroc, Feuille Bab el Mrouj – Taza Nord, échelle 1:50.000. Notes Mem Serv Géol Maroc 287.
Leblanc, D., 1978b. Carte Géologique du Maroc, Feuille Taineste, échelle 1:50.000. Notes Mem Serv Géol Maroc 305.
Leblanc, D., 1979. *Etude géologique du Rif externe oriental au Nord de Taza (Maroc)* (No. 281). Éditions du Service géologique du Maroc 281, 1–159.
Loget, N., Van Den Driessche, J., 2006. On the origin of the Strait of Gibraltar. Sediment. Geol. 188, 341–356.
Longhitano, S.G., 2013. A facies-based depositional model for ancient and modern, tectonically–confined tidal straits. Terra Nova 25 (6), 446–452.
Lourens, L., Hilgen, F.J., Laskar, J., Shackleton, N.J., Wilson, D., 2004. The Neogene Period. In: Gradstein, F., Ogg, J., Smith, A. (Eds.), A Geologic Time Scale. Cambridge University Press, London, pp. 409–440.
Lugli, S., Roveri, M., Schreiber, C.B., 2010. The Primary Lower Gypsum in the Mediterranean: a new facies interpretation for the first stage of the Messinian Salinity Crisis. Palaeogeogr. Palaeoclimatol. Palaeoecol. 297 (1), 83–99.
Manzi, V., Gennari, R., Hilgen, F., Krijgsman, W., Lugli, S., Roveri, M., Sierro, F.J., 2013. Age refinement of the Messinian Salinity Crisis onset in the Mediterranean. Terra Nova 25 (4), 315–322.
Martín, J.M., Braga, J.C., Betzler, C., 2001. The Messinian Guadalhorce corridor: the last northern, Atlantic–Mediterranean gateway. Terra Nova 13, 418–424.
Martín, J.M., Braga, J.C., Aguirre, J., Puga-Bernabéu, Á., 2009. History and evolution of the North-Betic Strait (Prebetic Zone, Betic Cordillera): a narrow, early Tortonian, tidaldominated, Atlantic–Mediterranean marine passage. Sediment. Geol. 216 (3–4), 80–90.
Martín, J.M., Puga-Bernabéu, Á., Aguirre, J., Braga, J.C., 2014. Miocene AtlanticMediterranean seaways in the Betic Cordillera (southern Spain). Rev. Soc. Geol. Esp. 27, 175–186.
Morel, J.L., 1989. Etats de contrainte et cinématique de la chaîne rifaine (Maroc) du Tortonien à l'actuel. Geodin. Acta 3, 283–294.
Morley, C.K., 1987. Origin of a major cross-element zone: Moroccan Rif. Geology 15, 761–764.
Morley, C.K., 1988. The Tectonic Evolution of the Zoumi Sandstone, Western Moroccan Rif. J. Geol. Soc. Lond. 145, 55–63. http://dx.doi.org/10.1144/gsjgs.145.1.0055.
Morley, C.K., 1992. Tectonic and sedimentary evidence for synchronous and out-of-sequence thrusting, Larache-Acilah area, Western Moroccan Rif. J. Geol. Soc. Lond. 149, 39–49. http://dx.doi.org/10.1144/gsjgs.149.1.0039.
Morley, C.K., 1993. Discussion of origins of hinterland basins to the Rif-Betic Cordillera and Carpathians. Tectonophysics 226, 359–376. http://dx.doi.org/10.1016/0040-1951(93)90127-6.
Mulder, T., Faugères, J.C., Gonthier, E., 2008. Mixed turbidite–contourite systems. Dev. Sedimentol. 60, 435–456.
Mutti, E., Tinterri, R., Benevelli, G., di Biase, D., Cavanna, G., 2003. Deltaic, mixed and

turbidite sedimentation of ancient foreland basins. Mar. Pet. Geol. 20, 733–755.
Nachite, D., Bekkali, R., Rodriguez-Lazaro, J., Martín-Rubio, M., 2003. Los ostracodos lacustres del Plioceno superior de la cuenca de Saïss (Norte de Marruecos): principales caracteristicas paleoambientales. Geogaceta 34, 95–98.
Parnell-Turner, R., White, N., Henstock, T., Murton, B., Maclennan, J., Jones, S.M., 2014. A continuous 55-million-year record of transient mantle plume activity beneath Iceland. Nat. Geosci. 7, 914–919.
Pérez-Asensio, J.N., Aguirre, J., Schmiedl, G., Civis, J., 2012. Messinian palaeoenvironmental evolution in the lower Guadalquivir Basin (SW Spain) based on benthic foraminifera. Palaeogeogr. Palaeoclimatol. Palaeoecol. 326, 135–151.
Platt, J.P., Allerton, S., Kirker, A., Mandeville, C., Mayfield, A., Platzman, E.S., Rimi, A., 2003. The ultimate arc: differential displacement, oroclinal bending, and vertical axis rotation in the External Betic-Rif arc. Tectonics 22 (3).
Potter, P.E., Szatmari, P., 2009. Global Miocene tectonics and the modern world. Earth Sci. Rev. 96 (4), 279–295.
Pratt, J.R., Barbeau, D.L., Izykowski, T.M., Garver, J.I., Emran, A., 2016. Sedimentary provenance of the Taza-Guercif Basin, South Rifean Corridor, Morocco: implications for basin emergence. Geosphere 12 (1), 221–236.
Rabaté, J., 1965. Paléogéographie de la zone sableuse du Vindobonien inférieur à la bordure méridionale de la plaine du Rharb. In: Report BRPM.
Rabaté, J., 1971. Etude des sables du Miocène terminal du Rharb. In: Report BRPM.
Reading, H.G., Collinson, J.D., 1996. Clastic coasts. In: Reading, H. (Ed.), Sedimentary Environments: Processes, Facies and Stratigraphy, 3rd ed. vol. 1996. Wiley-Blackwell, pp. 154–231.
Roest, W.M.J., 2016. Kinematic analysis of the last phases of deformation in north Morocco since the Mesozoic era. In: Master Research Project. Universiteit Utrecth–Vrije Universiteit Amsterdam (p. 70).
Rogerson, M., Schönfeld, J., Leng, M.J., 2011. Qualitative and quantitative approaches in palaeohydrography: a case study from core-top parameters in the Gulf of Cadiz. Mar. Geol. 280 (1), 150–167.
Rogerson, M., Bigg, G.R., Rohling, E.J., Ramirez, J., 2012. Palaeoceanography of the Atlantic-Mediterranean exchange: overview and first quantitative assessment of climatic forcing. Rev. Geophys. 50.
Rögl, F., 1999. Mediterranean and Paratethys. Facts and hypotheses of an Oligocene to Miocene paleogeography (short overview). Geol. Carpath. 50, 339–349.
Roldán, F.J., Galindo-Zaldívar, J., Ruano, P., Chalouan, A., Pedrera, A., Ahmamou, M., Ruiz-Constán, A., de Galdeano, C.S., Benmakhlouf, M., López-Garrido, A.C., Anahnah, F., 2014. Basin evolution associated to curved thrusts: the Prerif Ridges in the Volubilis area (Rif Cordillera, Morocco). J. Geodyn. 77, 56–69.
Roure, F., 2008. Foreland and Hinterland basins: what controls their evolution? Swiss J. Geosci. 101, 5–29.
Roveri, M., Lugli, S., Manzi, V., Schreiber, B.C., 2008. The Messinian Sicilian stratigraphy revisited: new insights for the Messinian Salinity Crisis. Terra Nova 20 (6), 483–488.
Roveri, M., Flecker, R., Krijgsman, W., Lofi, J., Lugli, S., Manzi, V., Sierro, F.J., Bertini, A., Camerlenghi, A., De Lange, G.J., Govers, R., Hilgen, F.J., Hübscher, C., Meijer, P., Stoica, M., 2014. The Messinian Salinity Crisis: past and future of a great challenge for marine sciences. Mar. Geol. 352, 25–58.
Saint-Martín, J.P., Charrière, A., 1989. Les édifices coralliens marqueurs de l'évolution paléogéographique en bordure du Moyen Atlas (Maroc). Sci. Geol. Mem. 84, 83–94.
Saint-Martín, J.-P., Cornée, J.-J., 1996. The Messinian reef complex of Melilla, northeastern Rif, Morocco. In: Franseen, E.K., Esteban, M., Ward, W.C., Rouchy, J.M. (Eds.), Models for Carbonate Stratigraphy from Miocene Reef Complexes of Mediterranean Regions. vol. 5. Society of Economic Paleontologists and Mineralogists, Concepts in Sedimentology and Palaeontology, pp. 227–237.
Samaka, F., Benyaich, A., Dakki, M., Hcaine, M., Bally, A.W., 1997. Origine et inversion des bassins miocènes supra-nappes du Rif central (Maroc). Etude de surfaces et de subsurface. Exemple des bassins de Taounate et de Tafrant. Geodin. Acta 10, 30–40.
Sani, F., Zizi, M., Bally, A.W., 2000. The Neogene–Quaternary evolution of the Guercif Basin (Morocco) reconstructed from seismic line interpretation. Mar. Pet. Geol. 17 (3), 343–357.
Sani, F., Del Ventisette, C., Montanari, D., Bendkik, A., Chenakeb, M., 2007. Structural evolution of the Rides Prerifaines (Morocco): structural and seismic interpretation and analogue modelling experiments. Int. J. Earth Sci. 96, 685–706.
Santisteban, C., Taberner, C., 1983. Shallow marine and continental conglomerates derived from coral reef complexes after desiccation of a deep marine basin: the Tortonian–Messinian deposits of the Fortuna basin, SE Spain. J. Geol. Soc. 140, 401–411.
Schönfeld, J., 1997. The impact of the Mediterranean Outflow Water (MOW) on benthic foraminiferal assemblages and surface sediments at the southern Portuguese continental margin. Mar. Micropaleontol. 29 (3), 211–236.
Schönfeld, J., 2002. Recent benthic foraminiferal assemblages in deep high-energy environments from the Gulf of Cadiz (Spain). Mar. Micropaleontol. 44 (3), 141–162.
SCP/ERICO report, 1991. Etude de synthèse géologique et géophysique du bassin du Gharb. In: ONHYM Internal Report, London, (533 pp.).
Sierro, F.J., 1985. The replacement of the "Globorotalia menardii" group by the Globorotalia miotumida group: an aid to recognizing the Tortonian/Messinian boundary in the Mediterranean and adjacent Atlantic. Mar. Micropaleontol. 9 (6), 525–535.
Sierro, F.J., Flores, J.A., Civis, J., Gonza, J.A., France, G., 1993. Late Miocene globorotaliid event-stratigraphy and biogeography in the NE-Atlantic and Mediterranean. Mar. Micropaleontol. 21 (1), 143–167.
Sierro, F.J., Hilgen, F.J., Krijgsman, W., Flores, J.A., 2001. The Abad composite (SE Spain): a Messinian reference section for the Mediterranean and the APTS. Palaeogeogr. Palaeoclimatol. Palaeoecol. 168, 141–169.
Simon, D., Meijer, P., 2015. Dimensions of the Atlantic–Mediterranean connection that caused the Messinian Salinity Crisis. Mar. Geol. 364, 53–64.
SOQUIP report, 1990. Raport d'interpretation du bassin du Rharb et des Rides Prerifaines. In: ONHYM Internal Report, (353 pp.).
Sprovieri, M., Bellanca, A., Neri, R., Mazzola, S., Bonanno, A., Patti, B., Sorgente, R., 1999. Astronomical calibration of late Miocene stratigraphic events and analysis of precessionally driven paleoceanographic changes in the Mediterranean basin. Mem. Soc. Geol. Ital. 54, 7–24.
Stow, D.A.V., Faugères, J.C., 2008. Contourite facies and the facies model. Dev. Sedimentol. 60, 223–256.
Stow, D.A.V., Faugères, J.-C., Viana, A., Gonthier, E., 1998. Fossil contourites: a critical review. Sediment. Geol. 115, 3–31.
Suter, G., 1980. Carte géologique de la Chaine Rifaine, échelle 1:500.000. Ministére de l'Energie et des Mines du Maroc, Direction de la Géologie, Rabat. Notes Mem Serv Geol Maroc 245a.
Tachet des Combes, E., 1967. Essai de synthèse sur les formations du Néogène du Rharb et de son pourtour. In: Internal Report BRPM – PETROFINA.
Tachet des Combes, E., 1971. Essai de reinterpretation de la sédimentation du Miocène du bassin du Rharb et de son pourtour. In: Internal Report BRPM – PETROFINA.
Taltasse, P., 1953. Recherches géologiques et hydrogéologiques dans le Bassin lacustre de Fès-Meknès. Notes et Memoires du Service Géologique du Maroc 115, 1–300.
Topper, R.P.M., Flecker, R., Meijer, P., Wortel, M.J.R., 2011. A box model of the Late Miocene Mediterranean Sea: implications from combined 87Sr/86Sr and salinity data. Paleoceanography 26 (PA3223).
Tinterri, R., 2011. Combined flow sedimentary structures and the genetic link between sigmoidal-and hummocky-cross stratification. GeoActa 10, 43–85.
Tulbure, M.A., Capella, W., Barhoun, N., Flores, J.A., Hilgen, F.J., Krijgsman, W., Kouwenhoven, T., Sierro, F.J., Yousfi, M.Z., 2017. Age refinement and basin evolution of the North Rifian Corridor (Morocco): No evidence for a marine connection during the Messinian Salinity Crisis. Palaeogeogr. Palaeoclimatol. Palaeoecol. 485, 416–432.
Turco, E., Bambini, A.M., Foresi, L., Iaccarino, S., Lirer, F., Mazzei, R., Salvatorini, G., 2002. Middle Miocene high-resolution calcareous plankton biostratigraphy at Site 926 (Leg 154, equatorial Atlantic Ocean): palaeoecological and palaeobiogeographical implications. Geobios 35, 257–276.
Van Assen, E., Kuiper, K.F., Barhoun, N., Krijgsman, W., Sierro, F.J., 2006. Messinian astrochronology of the Melilla Basin: stepwise restriction of the Mediterranean-Atlantic connection through Morocco. Palaeogeogr. Palaeoclimatol. Palaeoecol. 238 (1–4), 15–31.
Van der Schee, M., van den Berg, B.C.J., Capella, W., Simon, D., Sierro, F.J., Krijgsman, W., 2018. New Age Constraints on the Western Betic Intramontane Basins: A Late Tortonian Closure of the Guadalhorce Corridor? Terranova (in press).
Van Hinsbergen, D.J.J., Vissers, R.L.M., Spakman, W., 2014. Origin and consequences of western Mediterranean subduction, rollback, and slab segmentation. Tectonics 33, 393–419.
Vergés, J., Fernàndez, M., 2012. Tethys–Atlantic interaction along the Iberia–Africa plate boundary: the Betic–Rif orogenic system. Tectonophysics 579, 144–172.
Vidal, J.C., 1979a. Carte Géologique du Maroc, Feuille Tahala, échelle 1:50.000. Notes Mem Serv Géol Maroc 282.
Vidal, J.C., 1979b. Carte Géologique du Maroc, Feuille Dhar Souk, échelle 1:50.000. Notes Mem Serv Géol Maroc 298.
Wernli, R., 1988. Micropaléontologie du Néogene post-nappe du Maroc septentrional et description systématique des Foraminiféres planctoniques. Notes et Memoires du Service Geologique du Maroc(331) (p. 270).
Zizi, M., 2002. Triassic-Jurassic extensional systems and their Neogene reactivation in Northern Morocco (the Rides Prerifaines and Guercif basin). Notes Mem. Serv. Géol. Maroc 416, 1–138.
Zouhri, L., 2004. Structural evolution of the southern Rif Cordillera (Morocco): tectonics and synsedimentary fault processes. Geol. J. 39 (1), 81–93.
Zouhri, L., Lamouroux, C., Vachard, D., Pique, A., 2002. Evidence of flexural extension of the Rif foreland: the Rharb-Mamora basin (northern Morocco). Bull. Soc. Geol. Fr. 173 (6), 509–514.